Publication No. 05-063-205

MEASUREMENT OF THE ENERGY SPECTRUM OF GAMMA-EMITTING RADIONUCLIDES IN WORK AREAS TO DETERMINE REM PER ROENTGEN DOSE CONVERSION FACTORS FOR THE PHOSPHATE INDUSTRY

Prepared by
Florida International University

under a grant sponsored by

FIPR
Florida Institute of Phosphate Research

January 2004

The Florida Institute of Phosphate Research was created in 1978 by the Florida Legislature (Chapter 378.101, Florida Statutes) and empowered to conduct research supportive to the responsible development of the state's phosphate resources. The Institute has targeted areas of research responsibility. These are: reclamation alternatives in mining and processing, including wetlands reclamation, phosphogypsum storage areas and phosphatic clay containment areas; methods for more efficient, economical and environmentally balanced phosphate recovery and processing; disposal and utilization of phosphatic clay; and environmental effects involving the health and welfare of the people, including those effects related to radiation and water consumption.

FIPR is located in Polk County, in the heart of the central Florida phosphate district. The Institute seeks to serve as an information center on phosphate-related topics and welcomes information requests made in person, or by mail, email, or telephone.

Florida Institute of Phosphate Research
1855 West Main Street
Bartow, Florida 33830
(863) 534-7160
Fax: (863) 534-7165
http://www.fipr.state.fl.us

MEASUREMENT OF THE ENERGY SPECTRUM OF GAMMA-EMITTING RADIONUCLIDES IN WORK AREAS TO DETERMINE REM PER ROENTGEN DOSE CONVERSION FACTORS FOR THE PHOSPHATE INDUSTRY

FINAL REPORT

Hans Weger, Rajiv Srivastava, and M. A. Ebadian
Hemispheric Center for Environmental Technology
FLORIDA INTERNATIONAL UNIVERSITY
10555 West Flagler Street, TEC 2100
Miami, FL 33174

with

Thomas McNally, Robert Ammons, and J. Wesley Nall
POLK COUNTY HEALTH UNIT
225 Ave. D, NW
Winter Haven, FL 33881

Prepared for

FLORIDA INSTITUTE OF PHOSPHATE RESEARCH
1855 West Main Street
Bartow, Florida 33830

Contract Manager: Brian K. Birky, Ph.D.
FIPR Project Number: 02-05-063

January 2004

DISCLAIMER

The contents of this report are reproduced herein as received from the contractor. The report may have been edited as to format in conformance with the FIPR *Style Manual*.

The opinions, findings and conclusions expressed herein are not necessarily those of the Florida Institute of Phosphate Research, nor does mention of company names or products constitute endorsement by the Florida Institute of Phosphate Research.

PERSPECTIVE

Brian K. Birky, Ph.D., Public and Environmental Health Research Director

The Florida Institute of Phosphate Research (FIPR) established a framework to conduct research that will meet the needs of the people of Florida, which was published as *1998-2003 Strategic Research, Programmatic & Management Priorities*. Under the strategic research area of public health, the objective is to define the magnitude of public and occupational health aspects of radiation, hazardous or toxic materials, and air and water pollutants. One approach to meeting that objective is to conduct and sponsor studies of chemical and radiological contaminants in air, water and soil to determine if there are significant risks to public health for persons residing in phosphate regions. This research originated within and was conducted under that Strategic Plan.

Radioactivity is a natural part of the environment in which we live. Over the millennia, radioactivity has accumulated deep underground where phosphate ore is found. The radioactivity is more concentrated near the ore deposits than in surface soil, but the concentration varies such that there is less in North Florida ore than Central Florida ore. There are many radioactive elements from uranium to lead, and many different forms (isotopes) of those elements. When the ore is handled during beneficiation, the process in which phosphate rock is separated from clay and sand, the radioactivity concentrations in the rock concentrate that goes on for further processing is very similar to the concentrations in the original ore that was mined. At the chemical processing plant, that rock is reacted with acids and filtered. It is here, during the production of phosphoric acid and granulated fertilizers, that the different radioactive elements may be separated and concentrated, especially uranium and radium. Like many non-radioactive elements, radioactivity may become imbedded in equipment or form scale precipitates on pipes or other objects. Radium scale in particular can build up to where radiation levels on site are of concern.

Routine daily exposures of phosphate industry personnel to ionizing radiation are measured using badge dosimeters worn on the chest and processed by dosimetry vendors. However, there are other situations in which hand-held survey instruments are used to assess exposures to personnel or potential exposures to the public. The most common categories of survey instruments used in the phosphate industry are the solid scintillation (sodium iodide crystal) design and the gas-filled chamber design. These instruments are not very accurate when used to measure low-energy gamma radiation as is typical of environmental settings. This study evaluated the most common makes and models of survey instruments used in the phosphate industry in comparison to a broad energy germanium gamma spectrometer. This instrument is capable of quantifying gamma emissions by energy. It is possible to convert these measurements to the amount of ionization taking place in the exposed air, and to a human radiation dose at that location. Intercomparison of this spectrometer and the survey meters yields the conversion factors needed to properly interpret the survey meter readings. The study shows that the true dose rate (microrem per hour) in the average phosphate industry TENORM setting is

from 40 to 45 percent of the survey meter reading in microroentgens per hour. What does this mean in practical terms? The dose limit to a member of the public in Florida is 100 millirem per year due to man's activities above natural background dose. As an example, an off-site release policy of 50 microrem per hour above background for radioactive objects is set to keep a member of the public to under 100 millirem total exposure over 2,000 hours in the year. That is: (50 microrem/hour) x (2,000 hours) = 100,000 microrem = 100 millirem. In the past, a survey meter reading of 50 microroentgens per hour was considered equal to this level. This research shows that a reading of 125 microroentgens per hour using a Ludlum Model 12-S meter is actually equivalent to a dose of 50 microrem per hour. In terms of worker doses previously calculated using this same instrument, they may have been overestimated by 60 percent.

Use of these new dose conversion factors produces more accurate dose estimates to industry employees and members of the public. If the Florida Department of Health accepts these results and amends its release policy accordingly, more materials having value could be recycled rather than being buried in phosphogypsum stacks.

ABSTRACT

Gamma-ray energy spectra were measured at three phosphate mines, three processing plants, and other off-site areas using a germanium spectrometer. Conversion factors to determine actual exposure from survey meter readings (Ludlum models 12-S and 2401-P) were calculated using the measured energy spectra and the energy-dependent response curves. Dose conversion factors (Roentgen-to-rem) using the energy spectra and the energy-dependent data published by the International Committee on Radiological Protection (ICRP) for six orientations of external exposure were also calculated. Aluminum oxide carbide and lithium fluoride dosimeters were evaluated at the filtration areas and rock storage tunnels of the phosphate chemical processing plants.

Conversion factors of measured to actual exposure for the Ludlum 12-S and 2401-P (calibrated with a ^{137}Cs source) are 0.55 ± 0.07 and 0.62 ± 0.06, respectively, averaged over the phosphate industry. The dose conversion factors of actual exposure to effective dose for the following orientations of external gamma irradiation to the body are 1.07 ± 0.04 antero-posterior, 0.89 ± 0.01 postero-anterior, 0.64 ± 0.01 right lateral, 0.69 ± 0.01 left lateral, 0.86 ± 0.02 rotational, and 0.73 ± 0.01 isotropic. Conversion factors of measured to actual dose (not including orientation of gamma radiation to the body) for the aluminum oxide dosimeter and the lithium fluoride dosimeter are 0.967 ± 0.012 and 0.918 ± 0.024, respectively, for the industry. The conversion factor to change the measured exposure of a survey meter to the effective dose is the product of the measured to actual exposure conversion factor and the dose conversion factor.

ACKNOWLEDGMENTS

The successful completion of this project would not have been possible without the help and cooperation of the following people and organizations. We would like to thank Brian Birky of the Florida Institute of Phosphate Research for his guidance, review of the equations used to calculate the conversion factors, and for lending us the use of the Ludlum 2401-P survey meter. We would also like to thank Tim King from the Florida Fish and Wildlife Conservation Commission, whose help was essential for obtaining measurements at the Tenoroc State Park. He accompanied us during our measurements to guide us through the back roads and trails of Tenoroc so that we could find the measurement spots and not become lost. We would like to thank three phosphate companies for their cooperation, assistance, and opening their facilities to us: Cargill Fertilizer, Inc.; CF Industries, Inc., and U.S. Agri-Chemicals. In addition, we would like to thank representatives from ICN, Landauer, and Ludlum for their quick and satisfactory responses to our questions, especially regarding energy response.

TABLE OF CONTENTS

TABLE OF CONTENTS (CONT.)

LIST OF FIGURES

Figure **Page**

LIST OF FIGURES (CONT.)

Figure **Page**

LIST OF TABLES

Table **Page**

LIST OF TABLES (CONT.)

Table **Page**

EXECUTIVE SUMMARY

A broad energy germanium (BEGe) gamma spectrometer was employed at sites in the phosphate industry and the surrounding area to measure in situ gamma energy spectra. Sites where measurements were recorded included phosphate chemical processing plants (phosphoric acid filter, rock tunnel, phosphogypsum stack, and reactor), phosphate mines (phosphate rock ore without overburden, rock concentrate spills, clay settling ponds, and sand tailings), reclaimed mining sites (Tenoroc State Park, Rolling Hills), and baselines (Winter Haven). At Tenoroc, an old sand tailings site, clay settling area, and rock piling area were all included in the study. Rolling Hills is a residential area built on a formerly mined and reclaimed site. Bradley Junction, a residential area built over phosphate deposits that were never mined (mineralized land), was included in the sampling design, as well as a baseline location in Winter Haven that is in the same county (Polk) as the other sites, but not considered mineralized and never mined. Exposure readings were also obtained at these sites using Ludlum 12-S and 2401-P survey meters. Exposure refers to the amount of ionization in air (usually recorded in terms of roentgens or micro-roentgens per unit time). Aluminum oxide carbide (AlO) dosimeters from Landauer and lithium fluoride (LiF) thermoluminescent dosimeters (TLD) from ICN were set up at the rock tunnel and filter areas at the chemical processing plants for 19 days. These dosimeters are processed by the vendors and measure the estimated radiation dose (usually in millirem) to a person wearing the dosimeter or a location that people occupy.

The gamma energy spectra and the response curves of the survey meters were used to calculate a meter conversion factor (M) that converts the measured exposure rates to actual exposure rates for each measurement site. Additionally, the response curves of the AlO and LiF dosimeters were used to calculate a conversion factor (M) of actual dose from measured dose for these dosimeters. Conversion factors from the International Commission on Radiological Protection (ICRP) (1996), derived from extensive Monte Carlo calculations for six different orientations of external gamma-ray irradiation, were used to calculate dose conversion factors (DCF) that convert actual exposure to effective dose. Dose conversion factors that convert measured exposure for the survey meters or measured dose from the dosimeters to effective dose can be determined by multiplying DCF by M of the appropriate detector. The conversion factors determined in this study are shown below. The value of M for the pressurized ion chamber is 1.107 ± 0.004.

Table 1. Values of M and Final Dose Conversion Factors for Measured Roentgen to Rem.

Values of M (Ratio of Actual Exposure to Measured Exposure)				
Grouping	12-S	2401-P	A1 dosimeter	LiF TLD
All	0.55 ± 0.09	0.60 ± 0.08	0.92 ± 0.02	0.96 ± 0.02
Baselines	0.58 ± 0.06	0.56 ± 0.06	0.91 ± 0.02	0.96 ± 0.01
All but baseline	0.55 ± 0.07	0.62 ± 0.06	0.92 ± 0.01	0.97 ± 0.01
Filter	0.57 ± 0.06	0.65 ± 0.04	0.93 ± 0.01	0.97 ± 0.01
Reactor	0.52 ± 0.02	0.59 ± 0.11	0.92 ± 0.01	0.96 ± 0.02
Self-absorbing	0.55 ± 0.06	0.62 ± 0.05	0.92 ± 0.01	0.97 ± 0.01
Stacks	0.57 ± 0.02	0.63 ± 0.02	0.92 ± 0.01	0.97 ± 0.01
Sand tailings	0.56 ± 0.01	0.62 ± 0.03	0.92 ± 0.01	0.97 ± 0.01
Rock pile	0.54 ± 0.05	0.62 ± 0.08	0.92 ± 0.01	0.96 ± 0.01
Rock conc. spill	0.58 ± 0.02	0.65 ± 0.01	0.93 ± 0.01	0.97 ± 0.01
Clay	0.53 ± 0.08	0.60 ± 0.07	0.92 ± 0.01	0.96 ± 0.01

Dose Conversion Factors (Ratio of Effective Dose to Actual Exposure) Independent of Survey Meter						
Grouping	AP	PA	RLAT	LLAT	ROT	ISO
All	1.08 ± .04	.89 ± .01	.64 ± .01	.69 ± .01	.87 ± .02	.73 ± .01
Baselines	1.08 ± .02	.90 ± .01	.65 ± .01	.70 ± .01	.87 ± .01	.73 ± .01
All but baseline	1.07 ± .04	.89 ± .01	.64 ± .01	.69 ± .01	.86 ± .02	.73 ± .01

Note: To obtain the dose conversion factor for measured exposure to effective dose, use the product of the dose conversion factor and M for that specific survey meter. The values for M are for survey instruments calibrated with a ^{137}Cs source.

The six irradiation geometries are anterior-to-posterior (AP), posterior-to-anterior (PA), lateral from the right side to the left side (RLAT), lateral from the left side to the right side (LLAT), rotational around the vertical axis (ROT), and isotropic incidence from all directions (ISO). When a person is standing on a large affected area like a dry clay pond site, sand tailings area, or reclaimed land, the ISO geometry is probably most appropriate. Under conditions of multiple surrounding sources and frequent worker movement, the ROT geometry may be more appropriate. Under conditions of a smaller fixed source and fairly constant worker position, one of the other geometries, e.g., AP for a worker facing a source, can be chosen.

One goal of this project was to help determine the cause for discrepancies between the expected and measured dosimeter response from Birky and others (1998). The ratio of the aluminum dosimeter over the PIC detector is 1.20 ± 0.013, which is lower than the measured value of 1.53 ± 0.88 from Birky and others (1998). The error range is two standard deviations. The response ratio of the AlO over the LiF dosimeter, using values for "all but baseline," is equal to 1.05, which is lower than the measured

value of 1.22 from Birky and others (1998). Sources of uncertainty include the change in the AlO dosimeter design by Landauer since the 1998 report and the proprietary algorithms used by the dosimeter vendor to determine the effective dose. The phosphate industry could use these results in private consultation with the dosimeter vendor to incorporate the measured gamma energy spectra into algorithms that account for the dosimeter energy-dependent response.

INTRODUCTION

OBJECTIVE

The objectives of the proposed study are to measure the gamma-ray energy spectra using a broad energy germanium (BEGe) gamma spectrometer and to determine the exposure and dose conversion factors for external gamma radiation applicable to work areas in the phosphate industry. The overall objective of the conversion factors is to transform readings from radiation survey meters used in the phosphate industry to actual exposure rates and effective doses.

PROJECT DESCRIPTION

Source and Magnitude of the Problem

Technologically Enhanced Naturally Occurring Radioactive Material (TENORM) in the phosphate mining and processing industry is due to the presence of naturally occurring radionuclides from the uranium, actinium, and thorium series in the phosphate rock ore (matrix). Processing the matrix and manufacturing product such as phosphoric acid results in the concentration of these radionuclides in specific locations and materials and a subsequent increased radiation field.

Process of Mining and Production

Before the subsurface phosphate rock ore is removed from the earth, the overburden is removed and placed aside for reclamation purposes later. The matrix is $CaF_2 \cdot 3Ca_3(PO_4)_2$ with clay and silica sand. It undergoes a process called beneficiation that separates the phosphate rock from the clay and the sand.

After the dragline mines the matrix, which consists of approximately equal parts sand, clay, and phosphate rock, it dumps it into a pit where high-pressure water guns create a slurry that is then pumped to the beneficiation plant. At the beneficiation plant, the sand and clay are separated from the phosphate.

The matrix is washed in a rotating drum screen, or trommel, to remove large particles greater than 2 inches (50.8 mm) in diameter. The fraction smaller than 2 inches (50.8 mm) is further washed to break up the larger particles. It is then screened at 0.75 inches (19 mm) and then at 0.04 inches (1 mm) to produce a slurry of particles less than 0.04 inches (1 mm), a pebble product of particles between 0.04 inches (1 mm) and 0.75 inches (19 mm), and waste particles larger than 0.75 inches (19 mm).

The waste from this step is piled at the mine site, along with the waste fraction of particles greater than 2 inches (50.8 mm) from the trommel step. The slurry of particles less than 0.04 inches (1 mm) is "deslimed," or run through a hydrocyclone to remove particles smaller than 105 μm, generating a waste clay (phosphatic clay) slurry of about 3% solids of fine particles less than 0.004 inches (105 microns), and sand-sized particles between 0.04 inches (1 mm) and 0.004 inches (105 μm) that is the "flotation feed."

The waste clay slurry is then pumped to a pond where the clay settles. As the clay settles, the water is recycled. After the settling pond is filled, it takes about 2-5 years for the top two to three feet of the settling area to dry and be able to support weight. The soil beneath the top crust, however, remains the consistency of pudding for many years. There is much research being done on ways to reclaim clay-settling areas, which cover about 40 percent of the land that has been mined.

After the clay is washed away from the phosphate, the sand and the sand-sized phosphate particles, also called the "flotation feed," are put through the flotation process, which uses chemicals, water, and physical force to separate the phosphate and sand from each other. The sand is then pumped back to the mine site to be used in reclamation.

In the end, the phosphate from the flotation process is transported, with the larger pebble product from the washing process, to the chemical processing plant where it is reacted with sulfuric acid to make phosphoric acid. The phosphoric acid is used to make fertilizers and other products. Low-grade phosphate rock is used for manufacturing phosphoric acid, and the high-grade rock is sent to rock storage and used to make granular triple superphosphate (GTSP), monoammonium phosphate (MAP), and diammonium phosphate (DAP).

The processed phosphate ore is loaded into trucks and transported to the chemical processing plants. Sulfuric acid is added to the phosphoric material in the reaction attack tank (or reactor) to digest it and produce phosphoric acid (H_3PO_4). The reactor is a steel vessel often inside a reinforced concrete, brick-lined, building and is designed to release the reaction heat, which brings the acidic solution to boiling, as vapor through a flash cooler, which produces condensation. The gypsum crystal in the resulting acid/crystal slurry is filtered out by either a tilting pan (Byrd) or table (auger) filter. The slurry is placed on top of the filter cloth, and the acid is pulled through the fabric using a vacuum. The resulting gypsum cake (calcium sulfate dihydrate) waste is disposed in a specified area called a stack, which is a hill of hardened gypsum (Birky and others 1998).

Radiation Exposures Along the Process

As shown in a previous literature summary (Birky and others 1998), uranium-238 (^{238}U) and radium-226 (^{226}Ra) are in radioactive equilibrium in the phosphate rock ore at ~38 pCi/g. The majority of the ^{226}Ra in the matrix remains in the gypsum (26 pCi/g average for central Florida) and is disposed in the gypsum stack. Radium that is not disposed in the gypsum stack precipitates out of the slurry and becomes concentrated in

the filtrate tank scale (384.8 pCi/g measured in one study, but likely to be quite variable) and sediment (84.1 pCi/g also measured in one study and likely to vary greatly). Therefore, the filter areas often have relatively high radiation fields. Only a small fraction of the radium is retained in the phosphoric acid, but it becomes more concentrated as the phosphoric acid becomes more concentrated through evaporating the water (5% acid has 0.1 pCi/g, 15% acid has 0.2 pCi/g, and 30% acid has 0.4 pCi/g).

The majority of the ^{238}U remains in the product and becomes more concentrated. Activity concentrations in rock and products are quite variable. Recent data from central Florida processing operations show MAP and DAP are radiologically similar, averaging about 59 pCi/g U-238 and <4 pCi/g Ra-226. GTSP, produced by reacting high-grade rock with phosphoric acid, gets an extra infusion of U and Ra to yield about 67 pCi/g U-238 and 18 pCi/g Ra-226. The primary product by far is DAP, followed by MAP, and to a much lesser extent, GTSP (Birky and others 1998).

Therefore, radiation exposure rates and effective doses are a concern for the health and safety of phosphate workers. Due to this concern, the Florida Institute of Phosphate Research (FIPR) issued a report in July 1998 (Birky and others 1998) concerning an extensive radiation survey of the phosphate mines and processing plants to determine the radiation exposures to and the doses of the workers. The report also provided recommendations on how to reduce these exposures. Measurements were performed by badging participants with LiF TLDs and AlO dosimeters over an extended period of time combined with time and motion studies in the mine area, rock area, phosphoric acid area, dry products area, and shipping/storage area of multiple facilities. Supporting contractors who service these companies were monitored both on- and off-site. These areas were occupied by operators performing various jobs and by maintenance personnel, supervisors, painters, machinists, consultants, hydro- and sand-blasters, welders, and others. Equipment taken out of service from phosphoric acid plants contains scales with high concentrations of radium-226 (^{226}Ra). This radiation source affects mainly on-site maintenance personnel, transportation workers, and service industry personnel. The highest radium concentrations are expected immediately below the filter in the filter pans (Birky and others 1998).

Thus, even though exposure rates are significantly lower at the distances from the source where the workers perform most of their duties, there are a number of locations where persons could receive excessive doses. The Florida State Department of Health, Bureau of Radiation Control regulations regarding radiation exposures state that all exposures be kept as low as reasonably achievable (ALARA principle), with social and economic factors taken into account, and that total effective dose limits for members of the public (100 mrem per year), persons who have not received formal radiation protection training, and occupational radiation workers (5000 mrem per year) are not exceeded. In the phosphate industry, radiation exposures are controlled by limiting occupancy in areas of relatively high exposure rates.

Radiation Exposure and Dose Uncertainties

In any plant handling radioactive materials, one of the major issues is to determine the effective dose received by workers. The quantities equivalent dose and effective dose are not directly measurable, but are obtained from other easily measured quantities and specific conversion factors. Survey instruments are used to measure the exposure, expressed in units of Roentgens (R). Dose is expressed in different units called rem, and readings in R need to be converted to rem to determine dose. A dose conversion factor (DCF) converts the R value measured by the survey meter to the effective dose in rem.

Dosimeters are another method to determine the dose equivalents received by personnel. The measurements from dosimeters are in rem, so there is no need for a DCF. However, measurements performed at a number of locations in the phosphate industry showed the TLD/survey meter (calibrated to a pressurized ion chamber) ratio to be 1.53 ± 0.44 mrem/mR (Birky and others 1998). This rem/R ratio or DCF is much higher than the values of 0.000 (at 0.01 MeV and PA geometry) to 1.28 (at 0.08 MeV and AP geometry, reported by the International Commission on Radiological Protection (ICRP 1987), in the gamma energy range of 0.01 to 2 MeV. This unusually high rem/R ratio can be due to over-response of the dosimeter, under-response of the survey meter, or a combination of both. Besides detector response, the absorption of radiation by the human body is also energy-dependent. For example, muscle is often used to calculate the equivalent dose to tissue, but for gammas at energy below 100 keV, bone absorbs more energy than muscle.

A study of the gamma energy distribution (spectrum) and its effect on the energy-dependent response of survey meters and dosimeters is required to obtain a more thorough understanding and more accurate conversion factors. These energy spectra can be obtained by in situ measurements of gamma radiation fields with a high-resolution gamma spectrometer. The gamma energy spectrum cannot be determined by knowing the radioisotopes available, even though the known energy and abundance of gamma-rays emitted by the radionuclides are known, since many of the gamma-rays will have reduced energy values due to interactions with different materials before entering the air and interacting with the detector. This is known as a degraded spectrum because many of the emitted gamma-rays have degraded energies.

SPECIFIC PROJECT GOALS

The goals of this project were to determine meter and dose conversion factors accurately for various locations in the phosphate industry. Accurate gamma energy spectra were measured using a field-deployable BEGe-based gamma spectrometer. Survey meter readings were also obtained for comparison. The gamma energy spectra were used, along with the energy-dependent response curve for each survey meter, to calculate conversion factors to convert the survey meter exposure reading to the actual exposure value. In addition, data from ICRP (1996) were used to calculate dose

conversion factors for the phosphate industry, which convert exposure to effective dose. The areas where gamma energy spectra were measured include:

- chemical processing plants - phosphoric acid filter, rock tunnel, gypsum stack, and reactor; and
- mining sites - phosphate rock ore without overburden, concentrated phosphate spill, clay settling ponds, and sand tailings.

Dosimeters will also be placed at locations identified during measurements to have a stable radiation field. The readings on these dosimeters will be compared to the survey meter readings and the calculated conversion factors. This information will be used to assist in determining the cause of the discrepancy between the expected and measured response for the AlO/LiF dosimeter ratio and the AlO/pressurized ion chamber ratio from Birky and others (1998).

IMPACT OF THIS STUDY

Accurate determination of exposure and dose conversion factors will enable:

- assessment of effective doses of the workers and the public;
- application by phosphate industry management of radiation exposure reduction principles to ensure that exposure is as low as reasonably achievable;
- demonstration to the regulatory agency that the exposure levels are within the prescribed limits; and
- generation of calibration factors for survey instruments and dosimeters that can be used for conversion of their readings to true effective doses, resulting in more accurate dose determinations.

BENEFIT TO THE STATE OF FLORIDA

The state of Florida requires data on radiation exposure rates from all institutions and plants using radioactive materials. It also requires data about annual exposures of workers and members of the public to ensure that the exposures comply with the regulations. The accurate determination of exposure and dose conversion factors for gamma radiation will reduce ambiguity and increase confidence in the accuracy of the effective dose measurements and calculations. This will provide the state of Florida with invaluable data for determining accurate doses.

LITERATURE REVIEW

Dose Calculations

The current method of assessing the effective dose from external radiation is by placing a personal dosimeter directly on the individual. Radiation survey meters are also used to measure the exposure rates in work areas. These instruments are usually calibrated with a cesium-137 source. Depending on the type of detector, detector size, and detector housing used, the instruments may show a reading higher or lower than the actual value when exposed to gamma radiation of different energies. That is, these instruments do not give true values of exposures for various gamma energies of interest.

The main interaction mechanism of gamma-rays with atoms of low atomic number is Compton scattering, which depends mainly on the electronic density of the absorbing medium. Assuming that the exposure is accurately known, the current practice of converting the exposure to equivalent dose in tissue (muscle) is to multiply it by a factor that is the ratio of electronic density (electrons per gram) in muscle to that in air ($3.28 \times 10^{23}/3.01 \times 10^{23}$ or 1.0897), which is applicable to Compton scattering. Thus, an exposure of 1 R = 87.7 ergs/gram in air (or 0.877 rad in air) = 87.7 x 1.0897 ergs/gram in tissue = 95.5 ergs/gram in tissue = 0.955 rad. Using a value of 1 for biological quality factor (or radiation weighting factor) gives 1 R = 0.955 rem ≈ 1 rem. This conversion factor is often used to convert exposure to dose (Cember 1987).

Another general dose conversion factor employed is derived from reports released by the United Nations Scientific Committee on the Effects of Atomic Radiation (UNSCEAR), which recommended a conversion factor of 0.7 rem effective dose equivalent for adults per 1 rad of external gamma radiation absorbed dose in air for environmental exposure to gamma rays. Using the conversion factor of 1 R = 0.877 rad in air, a DCF of 0.7 rem/rad * 0.877 rad/R = 0.62 rem/R was calculated. This value was based on gonad dose measurements and the assumption that the doses in other significant organs are almost equal to the DCF of the gonads. The calculations were performed using the gamma energy spectrum expected in the environment (UNSCEAR 1977). However, in UNSCEAR (1988), the dose calculation methodology was changed to follow the definitions and units adopted in 1980 by the International Commission on Radiation Units and Measurements (ICRU) and to focus more on risk from radiation exposure. More recently, UNSCEAR (2000) no longer recommended the DCF value of 0.62 rem/R and instead employed the more rigorous definitions and calculations recommended by the ICRU and ICRP.

The dose conversion factors described above are general and based on simplifying assumptions. The ratio of equivalent dose to exposure (rem/R) for Compton scattering varies marginally over the energy range 0.1 to 10 MeV. However, for tissue or organs (e.g., bone) containing elements of higher atomic number and for different orientations of gamma-rays striking a person (particularly for low gamma-ray energies), the ratio of rem/R values (ICRP 1996) varies by a large factor from the value of 1 used as a rough

approximation (Cember 1987). Thus, even if the exposure rate is accurately measured, it does not accurately represent the effective dose rate to which workers are exposed.

Based on rigorous calculations, the ICRP (1987) has published the rem/R conversion factors for various gamma-ray energies and orientations. The data from ICRP (1996) are for an idealized human body without regard to gender, body fat content, height, or body position (such as sitting or standing). Los Alamos National Laboratory (Ennis and Trubey 1992) has developed a computer program, UNGER, for calculating effective gamma-ray equivalents for specific radionuclides. Kim and others (1998), Saito and others (1991 and 1998), Zankl and others (1992, 2002), and Han and others (1999) have published values of rem/R for various source orientations and gamma-ray energies based on Monte Carlo calculations. Zankl and others (2002) calculated the coefficients for idealized geometries and different adult male and female voxel models. Dose difference among the different voxel models ranged from 30% for some organs in the energy range of 60 to 200 keV and up to 100% for certain statures and differences in individual anatomical details. At low photon energies, the differences could be in the hundreds of percentage. These publications provide values derived by computations, not actual measurements.

Though not based on actual measurements, these derived conversion factors can be used along with the gamma energy spectra to determine site-specific DCFs. For sources without a degraded spectrum, dose calculations that could be used anywhere would be easy to calculate (provided the number of gamma-rays emitted are few for the parent and daughter radionuclides). A degraded spectrum from a source would arise if the source were behind a shield or other material that reduces the energy of some or most of the gammas due to interactions. For a degraded spectrum, either extensive calculations or measuring the gamma energy spectrum would be required to calculate a site-specific DCF that would not be applicable to other locations and other gamma radiation fields.

Another development is from Tsutsumi and others (2000), who have developed a sodium iodide detector that can directly measure the effective dose from the gamma energy spectrum measured by the detector.

Exposure and Dose Studies of TENORM Industries

Exposure and dose evaluations of other industries with TENORM have been examined. Measurements employing survey meters, smears, and other techniques were performed for the oil and gas industry (Smith and others 1996). Other studies performed have employed gamma spectrometers for depleted uranium in the environment from military activities (Anagnostakis and others 2001), in marbles and granites (El-Dine and others 2001), in the United Kingdom (Hipkin and others 1998), and in the oil and gas industry (Hamlat and others 2001). The gamma energy spectrum was used only for radionuclide identification or calculation of radioisotope concentration. None of these studies measured the energy spectrum for purposes of calculating accurate dose conversion constants as performed in this report.

METHODOLOGY

A BEGe gamma spectrometer was transported to three phosphate mines and three phosphate chemical processing plants to measure the gamma energy spectra. The gamma spectrometer also measured the gamma energy spectra at Tenoroc Park, Bradley Junction, Rolling Hills, and Winter Haven. The energy spectra data files were imported to an Excel spreadsheet where the calculations were performed. Survey meters, Ludlum models 2401-P and 12-S, were used alongside the gamma spectrometer to obtain exposure readings. AlO dosimeters from Landauer and LiF TLDs from ICN were obtained and placed in the rock tunnel and filter area at the three chemical processing plants. These locations were chosen since they have a stable radiation field. These dosimeters were retrieved after 19 days and sent to the vendor for processing.

Response curves from Ludlum for the 12-S and 2401-P, from ICN on the LiF TLD, and from Landauer on the AlO dosimeter were obtained and reduced to a series of equations that were placed into the Excel spreadsheet. The response curves and the gamma spectra were used to calculate the conversion factor to convert the measured exposure (or dose) to the actual exposure (or dose) for each measurement site for the survey meters (or dosimeters). Data from ICRP (1996) that convert photon flux to air kerma and that convert air kerma to effective dose for a range of gamma energy values were used along with the gamma spectra to calculate DCFs for each measurement site and external gamma-ray orientation.

RADIATION DETECTORS

Several radiation detectors were used in this study: BEGe gamma spectrometer, radiation survey meters, and dosimeters. Gamma spectrometers measure the energy distribution and the number of photons of the gamma radiation field. Survey meters are hand-held, light and enable a person to obtain a quick reading of the radiation exposure. However, survey meters measure only the total energy of the radiation field, not the energy distribution. Dosimeters are badges worn by a person during work hours to measure the dose he received during a period of time (monthly, quarterly, annually). Dosimeters only measure the total energy absorbed due to radiation but express it as a dose to the body (rem). Radiation survey meters and dosimeters are the instruments used in most industries involved with radioactive material. Gamma spectrometers are mainly used in scientific studies or to identify the radionuclides present and their concentration in waste, other materials, or in contaminated facilities or land.

Radiation survey meters are often calibrated at a specific gamma photon energy using a NIST-traceable radioisotope source. Survey meters, however, have a response that is dependent on the energy of the gamma-ray. The meter, if used to measure a radiation field in which the gamma-rays are at a different energy, will have a reading either higher or lower than the actual exposure.

Survey Meters

The Ludlum model 12-S, which uses a sodium iodide scintillator, and the model 2401-P survey meter (see Figure 1), which uses a pancake Geiger-Mueller tube, were chosen for this study since they are the two most commonly used survey meters in the phosphate industry. The Model 2401-P survey meter was borrowed from FIPR and was calibrated with a Cs-137 source. The Model 12S was borrowed from the Polk County Health Unit (PCHU) and calibrated with a Ra-226 source. The Model 12-S rate meter has X1, X10, X100, and X1000 multipliers, reading within plus or minus 10% of true value, and in units of 0 to 3 μR/hr. The Model 2401-P has X1, X10, X100 scaling and has a meter dial setting from 0 to 0.05 mR/hr. Both have a temperature range from –4ºF to 122ºF.

The response curves (Figures 2 and 3), normalized for Cs-137, were obtained from Ludlum (Ludlum 2002) and are for the photons per second detected at energy E per photon per second at energy E. The response curves are described as a series of equations (see Tables 2 and 3) to facilitate calculations in an Excel spreadsheet. These equations were generated, for the survey meters and dosimeters, by obtaining data points from the response curve graphs (using pencil and ruler) and inputting the data in an Excel spreadsheet for curve fitting. The equation for the 12-S from 0 to 60 keV was extrapolated from the data from 60 to 80 keV. Additionally, for the 12-S, the response for energy greater than 1200 keV was assumed to be constant at higher energies. The equation for the 2401-P from 0 to 16 keV was extrapolated using data from 16 to 56 keV and is assumed to be 1.0 from 0 to 12 keV to prevent the inverse response curve approaching infinity as the response curve approached zero. The response curve beyond 1260 keV is extrapolated from data from 200 to 1260 keV. The 2401-P admits beta particles into its sensitive volume and responds to them with a detection efficiency that differs than that for gamma radiation. Due to the short range of beta particles, they are not considered in this analysis, because most would be absorbed in the source material itself or attenuated in air prior to reaching the sensitive detector volume.

Figure 1. The Ludlum 12-S and 2401-P Survey Meters (from Left to Right) Used in This Study.

Table 2. Equations Used to Calculate the Response Curve for the Ludlum 12-S Survey Meter.

Energy Range (keV)	Curve (Response = equation, where E is energy in keV)
0 – 64	0.05*E + 4
64 – 145	$5x10^{-7}*E^4 – 0.0002*E^3 + 0.0287*E^2 – 1.7442*E + 45.329$
145 – 339	-0.0189*E + 9.8873
339 – 557	-0.0092*E + 6.58
577 – 1200	$-4.84x10^{-9}*E^3 + 1.532x10^{-5}*E^2 – 0.0161*E + 6.409$
1200-	0.743

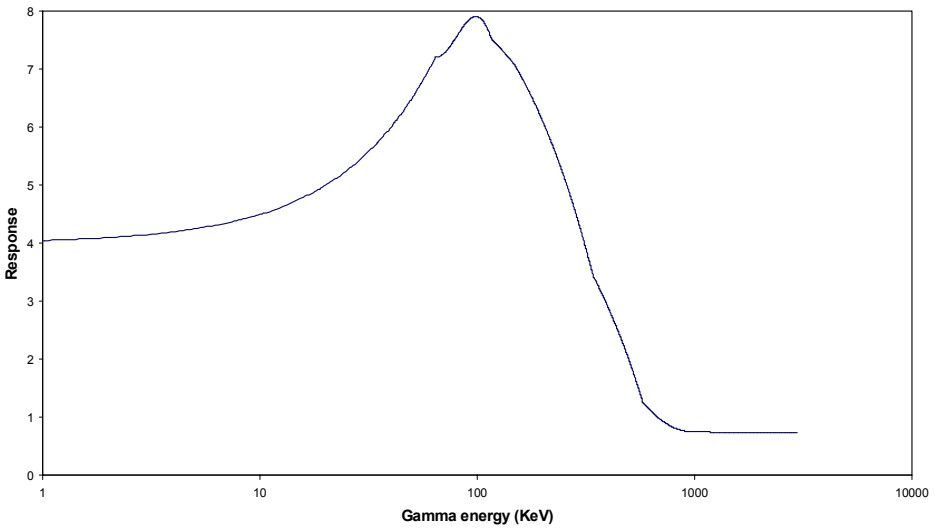

Figure 2. Response Curve, Normalized for Cs-137, Determined by the Equations in Table 2 for the Ludlum 12-S Survey Meter (Ludlum 2002).

Table 3. Equations Used to Calculate the Response Curve for the Ludlum 2401-P Survey Meter.

Energy Range (keV)	Curve (Response = equation, where E is energy in keV)
0 – 12	1.0
12 – 50	$0.1059*E - 0.2648$
50 – 88	$-0.0033*E^2 + 0.4359*E - 8.6719$
88 – 157	$25.457*e^{-0.0207*E}$
157 – 279	$-4.989x10^{-5}*E^2 - 2.447x10^{-2}*E + 3.598$
279 –3000	$9.0 \times 10^{-4}*E + 0.405$

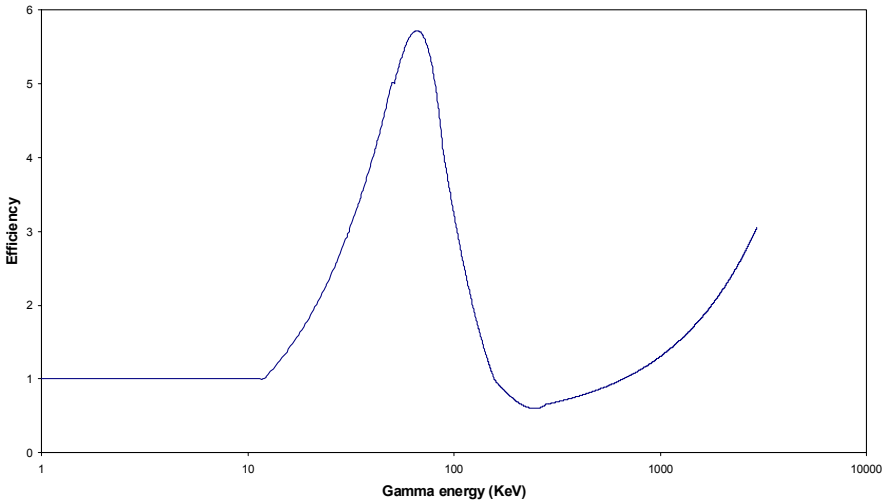

Figure 3. Response Curve, Normalized for Cs-137, Determined by the Equations in Table 3 for the Ludlum 2401-P Survey Meter (Ludlum 2002).

Dosimeters

Two different dosimeter types are commonly used in the phosphate industry: a lithium fluoride (LiF) thermoluminescent dosimeter (TLD) and an aluminum oxide (AlO) dosimeter. Both types were evaluated in this study.

The LiF TLD has a gamma radiation absorption response similar to human tissue for a wide energy range. The LiF TLDs from ICN Dosimetry Service used in this study can measure beta, gamma, and x-ray, and gamma radiation. The TLD contains three LiF thermoluminescent elements using ^{7}Li (for measuring deep dose, lens of eye, and shallow dose). A thin Mylar window allows low-energy beta radiation to be reported. Only deep dose is of interest in this study. The minimum reportable dose is 10 mrem, and the useful dose range is 10 mrem to 1000 rads.

A response curve (Figure 4) for the LiF TLD (relative deep dose equivalent for detector behind filters in holder) was obtained from ICN (ICN 2003). The response is expressed by several equations (Table 4) to facilitate use of this data in an Excel spreadsheet. The response was extrapolated to 0 keV using given data from 20 to 39 keV. The response was extrapolated beyond 639 keV using data from 129 to 639 keV and assumed to level out at 1.0.

Table 4. Equations Used to Calculate the Response Curve of the ICN LiF TLD.

Gamma Energy (keV)	Response Equation
0 to 39	-0.0832*E + 4.6632
39 to 76	-0.0068*E + 1.6864
76 to 129	-0.0017*E + 1.2974
129 to 639	-0.00016*E + 1.100
639 - 3000	1.0

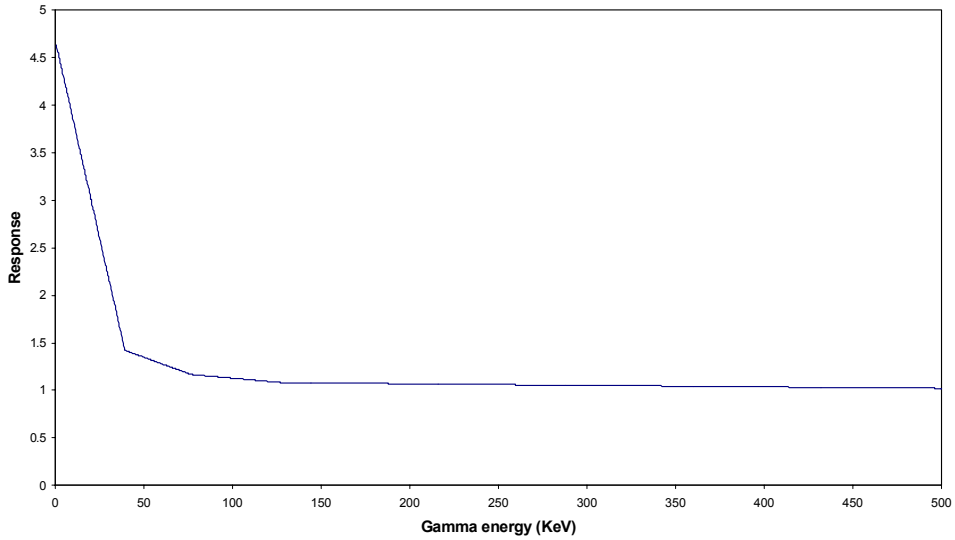

Figure 4. Response Curve Determined by the Equations in Table 4 for the ICN LiF TLD (relative deep dose equivalent for detector behind filters in holder).

Aluminum oxide dosimeters are more sensitive, rugged, and durable in the field than LiF TLDs. However, the energy response of the absorbed dose is not similar to human tissue and must be corrected. In the study by Birky and others (1998), both dosimeters were used to measure the absorbed dose. The ratio of the aluminum oxide dose over the LiF dose was 1.22.

The AlO dosimeter from Landauer was chosen for this study. It is capable of measuring x-rays, gamma-rays, and beta radiation. It has a minimal reporting value of 1 mrem with a precision of ± 1 mrem. The sensing material is a thin layer of aluminum oxide (Al_2O_3) and is read by optically stimulated luminescence. The dosimeter has a copper filter, open window, tin filter and imaging filter. One of the results from the Birky and others (1998) report is a response ratio of 1.53 for the AlO dosimeter values over the values obtained using a PIC. However, between 1998 and 2003, Landauer has issued a new AlO dosimeter called the Luxel and it became impossible to obtain the old model X9. Therefore, the response may have changed, and the AlO values obtained in this report may not be applicable to the results of Birky and others (1998).

The response of the dosimeter (Figure 5) was obtained from Landauer (2003) and is expressed as a series of equations (see Table 5) to facilitate use of this data in an Excel spreadsheet. The response is for relative deep dose equivalent for detector behind filters in holder. The response beyond 657 keV was extrapolated from given data at 115 to 657 keV.

Table 5. Equations Used to Calculate the Response Curve for the Aluminum Oxide Dosimeter from Landauer.

Gamma Energy (keV)	Response Equation
0 – 28	1.0
28 – 33	0.0114*E + 1.319
33 - 50	0.00571*E + 0.7547
50 – 69	0.00353*E + 1.216
69 – 115	0.0007174*E + 1.0225
115 -	0.0001476*E + 0.923

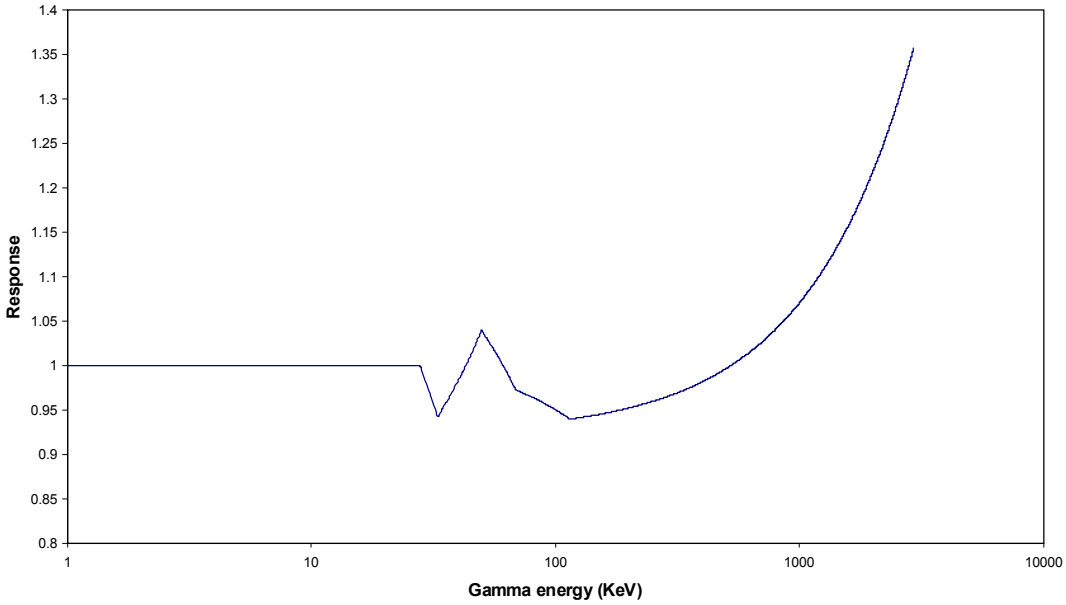

Figure 5. Response Curve Determined by the Equations in Table 5 for the Aluminum Oxide Dosimeter from Landauer (relative deep dose equivalent for detector behind filters in holder).

Pressurized Ion Chamber

The pressurized ion chamber (PIC) detector is not used for measuring radiation exposure but for calibrating the survey meters in the field. Therefore, the PIC meter was not evaluated in this report. However, the response curve is presented here to allow using these results to analyze the reason for a ratio of 1.53 for the AlO dosimeter value over the PIC value in Birky and others (1998). The response curve (Figure 6) was obtained from Figure 21 of Birky and others (1998). The equations used to calculate the response curve are shown in Table 6 (photons per second detected at energy E per photon per second at energy E) and for a calibration with a ^{137}Cs source. The values below 40 keV are assumed to be 0.1 to avoid dividing by zero.

Table 6. Equations Used to Calculate the Response Curve for the PIC.

Gamma Energy (keV)	Response Equation
0 – 40	0.1
40 - 90	1.865*ln(E) – 6.775
90 - 216	-0.00545*E + 2.091
216 - 3000	$3.846 \times 10^{-8} * x^2 - 9.231 \times 10^{-5} * E + 0.9308$

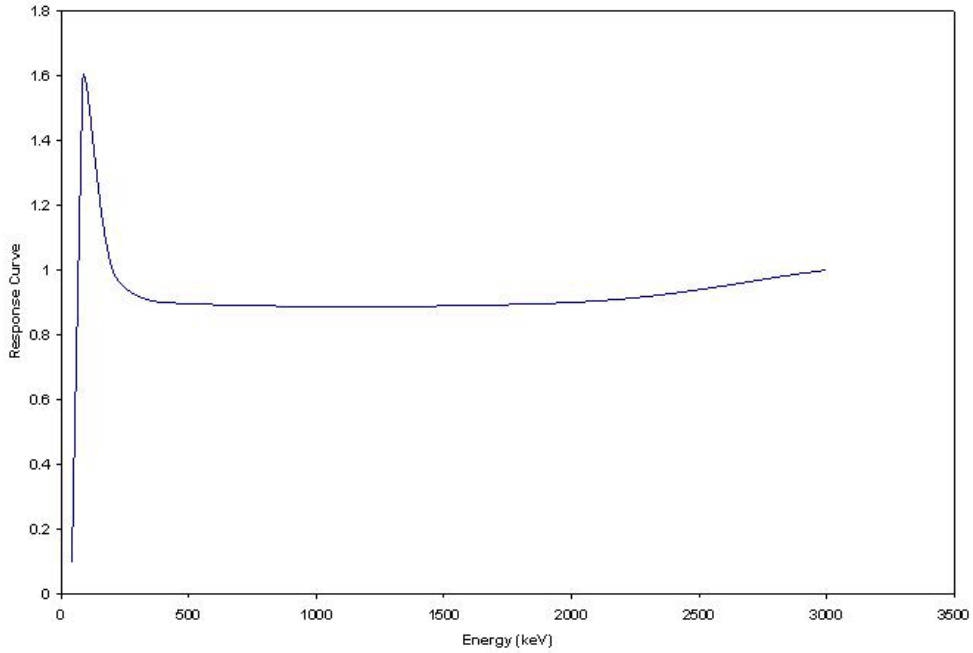

Figure 6. Response Curve Determined by the Equations in Table 6 for the Pressurized Ion Chamber.

Broad Energy Germanium (BEGe) Detector for Gamma Energy Spectroscopy

The gamma spectrometer used in this study is a broad energy germanium (BEGe) detector from Canberra, model BE3830. This detector has an active diameter of 70 mm, active area of 3800 mm^2, thickness of 30 mm, cryostat window thickness of 0.6 mm carbon composite, and bias voltage of 3000 V dc. The nominal efficiency of the detector is 34% with a resolution (in eV-FWHM) of 450 for a 5.9 keV photon, 750 for a 122 keV photon, and 2100 for a 1332 keV photon.

The BEGe detector is well suited for in situ measurements since it has enhanced low energy minimal detectable activities and good high-energy performance. The detector is placed on a wheel cart, allowing for easy transportation (see Figure 7). The detector can be moved to point from directly downwards to directly upwards. A battery-operated pointing laser is included on top of the detector to provide the ability to aim the detector accurately at the source.

Figure 7. The BEGe Detector, Pointed Downwards, with Laptop Computer at the Sand Tailings Area of Tenoroc State Park.

The detector contains a set of lead shields and collimators on the cart. The shielding (gray), which includes four front shields and one back shield (see Figure 8), completely surround the sensing element of the spectrometer. The back shield is behind the detector and is the fifth, larger gray shield in Figure 8. The shields have a cast aluminum exterior with baked epoxy coating to simplify decontamination and have 0º, 30º, 90º, and 180º collimator assemblies (see Figure 9) to minimize interference from other radiation sources and limit the detector's field of view. The 0º shield configuration is obtained by placing the shielding cap over the front shields, so that the sensing element is entirely shielded. The 30º view (detector only sees radiation at a 30º angle from the opening of the shielding in front) and 90º view are obtained by removing smaller lead shielding pieces from the front shield, revealing part of the surface of the detector's face. A 180º view is obtained by removing the first lead shield from the front. The face of the detector is about 1 mm behind the surface of the second shield to protect it.

Figure 8. Side View of the BEGe Detector to Allow Viewing the Shield Configuration.

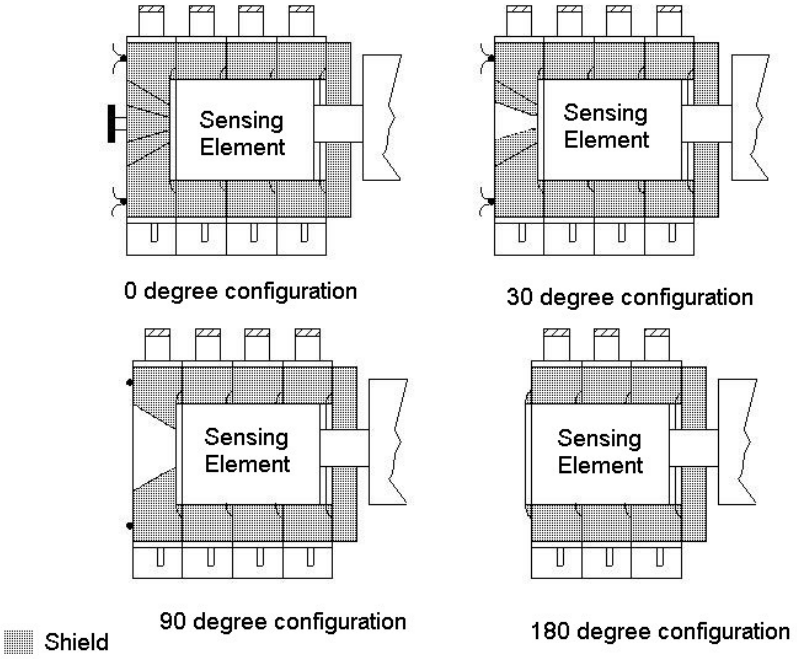

Figure 9. The Different Shielding Configurations for the BEGe Detector.

The thickness of the shielding was determined by Canberra (1) to maximize the shielding of radiation by increasing the thickness and (2) to minimize detecting cosmic rays that would result from the cosmic rays interacting with too thick a shield. X-rays that could be produced from radiation interactions with the lead were minimized by a lining of tin and copper. No cosmic radiation interference was measured, which was determined

by taking measurements with full (0 degrees) shielding configuration. Modern electronics now eliminate most problems with inaccurate counting that results from long counts such as gain shifts from changes in temperature or power voltage fluctuations.

The spectrometer requires liquid nitrogen to cool the detector head. A double-walled vacuumed Dewar that contains a 5.4-day supply of liquid nitrogen is situated behind the detector (see Figure 8: cylindrical shaped, with the Canberra name on it). The Dewar was filled in Miami before transporting the spectrometer for measurements. No more than three days of consecutive measurements were performed between Dewar fillings. The spectrometer will not turn on the high voltage bias if the temperature sensor detects too high of a temperature due to no liquid nitrogen in the Dewar.

The estimated weight of the detector is 18 lbs when empty, 30 lbs when full. Each front shield is approximately 43 lbs, and the back shield is 40 lbs. The total weight of the shielding is 212 lbs (Colaresi 2002). The detector was easy to move on level, hard surfaces, since it was placed on a wheeled cart. However, it was difficult, requiring at least two people, to move in mud or up and down a ramp. The detector was transported in a cargo van and required a metal ramp to move it onto or off the cargo van (see Figure 10). Sampling time during the day was limited by the amount of time required to load, unload, and move the detector into place. In accordance with Canberra's recommendations for operating the detector, the high voltage of the instrument was not activated until the relative humidity was below 80% (measured with a relative humidity meter) to prevent voltage leakage from damaging the machine. Therefore, measurements could not begin until about 10:00 a.m. on most days.

Figure 10. The Cargo Van Packed and Ready to Go with the Spectrometer and Ramp.

Each detector from Canberra was characterized in-house before shipment. The efficiency calibration curve (Equation 1 where Eff is the efficiency of the detector, E is the energy of the gamma-ray in keV, and ln(E) is the natural logarithm of the Energy) from 45 keV to 7 MeV was obtained using NIST-traceable sources and MCNP Monte Carlo modeling. The efficiency of the detector is a measure of the probability of a gamma-ray with a certain energy being detected by the spectrometer. Germanium detectors have good energy resolution compared to other spectrometers (such as sodium iodide) but have lower efficiencies. The spectrometer has 8,192 channels, each channel representing an energy range of gamma-rays detected. Equation 2 describes the energy per channel.

$$\ln(Eff) = -188.2 + 120.8 \ln(E) - 31.03 \ln(E)^2 + 3.722 \ln(E)^3 - 0.2006 \ln(E)^4 + 0.003406 \ln(E)^5 \quad (1)$$

$$E = -0.4187 \text{ keV} + 0.3595 \text{ keV/channel} \quad (2)$$

Throughout the duration of the project, a smoke detector with an Am-241 source at a strength of about 1 μCi was used as a radiation source to test the response of the detector. The typical Am source in a smoke detector (Am-241 in a gold matrix) is about 0.5 g and 3 to 5 mm in diameter. The main gamma-ray released by Am-241 is at 59.5 keV. Each measurement day, the gamma spectrometer measured the smoke detector to verify that the energies and efficiencies of the spectrometer remained the same.

EQUATIONS USED TO CALCULATE CONVERSION FACTORS

Units and Definitions

Radiation exposure is the amount of energy that the radiation transmits to a unit mass of air and is determined by measuring the amount of ionization, or ion pairs, produced by the radiation. Exposures to X-rays and gamma-rays are specified in SI units as exposure units (1 X unit = 1 C/kg air) and in older, more commonly used units as Roentgens (1 R = 1 statcoulomb/cm^3 in air at 0 ºC and 760 mm Hg). Absorbed dose is the amount of energy absorbed by a unit mass of material due to radiation. The SI unit for absorbed dose is the Gray (Gy), and the older, more commonly used unit is the rad, which stands for "radiation absorbed dose." A Gray is equal to 1 J/kg and to 100 rad. The effective and equivalent doses are two different measures of the amount of biological damage that the radiation imparts per unit mass of tissue or other organ. The units are expressed in the same units of energy over mass, but are multiplied by a biological quality factor. The SI units are Sieverts (Sv), and the older, more commonly used units are rems (1 Sv = 1 J/kg = 100 rem). A quality factor Q is used to convert from absorbed dose to effective dose, with the value of Q dependent on radiation type and energy (Cember 1987). In more modern terminology, Q is called the radiation weighting factor and is designated W_R.

The current practice of converting the exposure to equivalent dose in tissue (muscle) is to multiply it by a factor that is the ratio of electronic density (electrons per gram) in muscle to that in air ($3.28 \times 10^{23}/3.01 \times 10^{23}$, or 1.0897). This ratio is used since the main interaction mechanism of gamma-rays with atoms of low atomic number is Compton scattering, which depends mainly on the electronic density of the absorbing medium. Thus, 1 R = 87.7 ergs/gram in air (or 0.877 rad in air) = 87.7 x 1.0897 ergs/gram in tissue = 95.5 ergs/gram in tissue = 0.955 rad. Using a value of 1 for quality factor (or radiation weighting factor) gives 1 R = 0.955 rem ≈ 1 rem.

The ICRP (1977 and 1991) has defined various quantities, such as absorbed dose, equivalent dose (and dose equivalent), and effective dose (effective dose equivalent). The equivalent dose (H_T; see Equation 3) is calculated by multiplying the absorbed dose, which is averaged over a tissue or organ, and the radiation weighting factor (W_R) for each radiation exposure event. The value $D_{T,R}$ is the absorbed dose, averaged over tissue or organ T, due to radiation exposure event R (Shleien and others 1998).

$$H_T = \sum_R W_R D_{T,R} \tag{3}$$

The effective dose (H; see Equation 4 where W_T is the tissue weighting factor) is the sum of the weighted equivalent doses (obtained by multiplying tissue equivalent doses by tissue weighting factors) for various tissues that represent, in total, the human body. The effective dose is represented by E in the ICRP publications, but to avoid confusion with the use of E for gamma energy, the letter H is used.

$$H = \sum_T W_T \sum_R W_R D_{T,R} \tag{4}$$

The effective dose H has been tabulated for different gamma energies by ICRP (1996) for different irradiation geometries AP, PA, LAT, ROT, ISO, described below.

- Antero-posterior geometry (AP): Ionizing radiation strikes the body in an orthogonal direction to the person's long axis.
- Postero-anterior geometry (PA): Ionizing radiation strikes the back of the body in an orthogonal direction to the person's long axis.
- Right lateral geometry (RLAT): Ionizing radiation strikes the body on the right side in an orthogonal direction.
- Left lateral geometry (LLAT): Ionizing radiation strikes the body on the left side in an orthogonal direction.
- Rotational geometry (ROT): The body is irradiated by a parallel beam of ionizing radiation in an orthogonal direction to the person's long axis and rotates around the long axis at a uniform rate.
- Isotropic geometry (ISO): The body is irradiated by a radiation field in which the particle fluence per unit of solid angle is independent of direction.

Survey Meter Efficiency

Before proceeding to the equations used to calculate the conversion factor values, it is necessary to form equations to describe the survey meter efficiency and response curve. The response of the survey meter is the amount of energy registered by a detector for an absorbed photon in relation to the actual energy of the photon. If the response is 2 for a 100 keV gamma, then a 1 mR field of 100 keV gamma photons will be read as a 2 mR field, unless the survey meter was calibrated in a field of 100 keV gamma-rays. The response is related to the efficiency and therefore will be represented as Eff(E).

The survey meter is calibrated using a radioisotope of known strength, allowing the radiation exposure to be calculated. The survey meter is adjusted so that the reading equals the calculated exposure. However, the survey meter is calculated at only one gamma energy value, whereas the measured radiation fields will contain gamma-rays at different energies. The response of the phosphate industry to this problem is to calibrate the survey meters in actual workplace radiation fields against a PIC. The calibration, in effect, normalizes the response curve (Rsp(E) in Equation 5). The value Eff(E) is the efficiency curve before being normalized by calibrating the survey meter. The constant $Eff(E_c)$ is the efficiency at the gamma energy for which the survey meter was calibrated. The value of E_c = 662 keV is in Equation 5 since the Cs-137 source is often used for calibration, which emits only one gamma at 662 keV. The response values as a function of E are obtained by the vendor, who has characterized the meter's response to a range of different gamma energy values. For determining the response of a meter calibrated at a different energy (Rsp*) than Cs-137, Equation 6 can be used in which Rsp_n [$Rsp(E_n)$] is the response at the different gamma energy obtained from the response curve.

$$Rsp(E) = Eff(E)/Eff(E_c) = Eff(E)/Eff(E_c = 662\ keV) \qquad (5)$$

$$Rsp^*(E) = Rsp(E)*Rsp(E_n) = Rsp(E)/Rsp_n \qquad (6)$$

Calculating the value of Rsp_n needs to consider all of the gamma-rays present. Many calibration sources have only one predominant energy at which gamma-rays are emitted. The radioisotope most commonly used is Cs-137. Cesium-137 decays to the stable isotope Ba-137 with only one gamma-ray at 662 keV being emitted. If more than one gamma energy needs to be considered, Equation 7 should be used in which χ_m is the abundance (percentage) at which the gamma photon at energy E_m is emitted and A_j is the activity of radionuclide j. The equation is for more than one radioisotope present, which can arise for radiation sources in which the radioisotope decays to further gamma-emitting daughter radioisotopes. The energy of the emitted gamma photon acts as a weighting factor for this calculation.

$$Rsp_n = \frac{\sum_{j=1}^{j\max} \sum_{m=1}^{m\max} \chi_{j,m} Rsp(E_m) E_m A_j}{\sum_{j=1}^{j\max} \sum_{m=1}^{m\max} \chi_{j,m} E_m A_j} \qquad (7)$$

A radioactive source using Ra-226 will be considered since the survey meter 2401-P was calibrated using a tightly sealed ^{226}Ra source. The gammas emitted by Ra-226 are 390.7 keV at an abundance of 0.000067, 186.21 keV at 0.0328, 94.9 keV at 0.001357, 83.78 keV at 0.002994, 81.07 keV at 0.001802, and 11.7 keV at 0.008022 (RSA Publications 2000). The value for Rsp_n for using only the 186.21 keV gamma is 6.37 and for all the gammas emitted is 6.38. However, as seen in the results section, a response of 6.37 (compared to the response curve if calibrated with a Cs-137 source) compared to the 12-S survey meter, which was calibrated at Cs-137. What were not considered in the above calculation were the gamma-emitting daughters of Ra-226 (see Table 7). Since Rn-222 has a half-life that is much smaller than Ra-226, and Po-218, Pb-214, Bi-214 and Po-214 have half-lives much smaller than Rn-222, secular equilibrium is assumed for all the daughters of the Ra-226 source. Secular equilibrium indicates that the activities of the parent and the daughter radionuclides are equal. Using Equation 7, the value for Rsp_n is calculated to be 1.3, which agrees with the actual measurements obtained more than the value of 6.38.

Table 7. Daughter Radionuclides of Ra-226 (Half-Life of 1600 Years).

Radioisotope	Half-Life	Gammas Emitted	
		Energy (keV)	Abundance
Rn-222	3.8 days	512	0.00076
Po-218	3.05 minutes	none	
Pb-214	26.8 minutes	10.8 to 839.02	Total: 1.04
Bi-214	19.9 minutes	11.1 to 2447.9	Total: 1.36
Po-214	0.16 milliseconds	797.3	0.000104

(RSA Publications 2000)

Conversion of Measured Exposure to Actual Exposure

To convert the measured exposure of the survey meters to actual exposure, the gamma energy spectrum was measured using a BEGe gamma spectrometer. The data file generated by the spectrometer consists of the number of gamma photons counted in a narrow energy range (a channel). The total number of channels is 8,192 and covers the energy range of 0 to 2.944 MeV (no photons are counted by the detector in the channels from 0 to 3 keV). These data were then placed into an Excel spreadsheet, and the following equations were used to calculate the meter conversion factor M for that particular survey meter. The product of M and the survey meter reading will equal the actual exposure rate.

The exposure rate is represented by X, defined in Equation 8, where φ= photon flux in units of photons/cm^2-s = $N/T_m \cdot A_s$, N = number of photons, A_s = standard cross-sectional area, T_m = measurement time, E is the energy of the photon in units of MeV; 1.6 x 10^{-13} J/MeV is the conversion of MeV to joules; μ_a is the mass absorption coefficient of air for energy E in units of cm^2/g, and 34 (J/kg)/(C/kg) is the average energy dissipated in the production of a single ion pair in air.

$$X = \frac{\phi \cdot E \cdot 1.6x10^{-13}(J/MeV) \cdot \mu_a}{34(J/kg \,/\, C/kg)} \quad (8)$$

To simplify the equations, the constant c will be defined (Equation 9) to incorporate all of the constants in the exposure equation above as well as some unit conversion factors so that X is in units of R (1 R = 2.58 x 10^{-4} C/kg). The constant c is the conversion factor of MeV/g to R.

$$c = \frac{1.6x10^{-13} J/MeV \cdot 1000 g/kg}{2.58x10^{-4}(C/kg)/R \cdot 34(J/kg)/(C/kg)} = 1.824x10^{-8} \frac{g \cdot R}{MeV} \quad (9)$$

X_A is defined as the actual exposure rate (Equation 10) and X_R as the exposure rate read by the operator from the survey instrument (Equation 11). The letter m is the channel number, which ranges from 1 to 8192. The ratio M is defined in Equation 12, in which ψ_1 and ψ_2 are used to simplify the equations. The value of Rsp_n for a meter calibrated to Cs-137 would equal 1.0. The value X_R is calculated using X_A, determined using the measured gamma energy spectrum, and detector response curve supplied by the manufacturer.

$$X_A = \sum_{m=1}^{8192} E_m \cdot c \cdot \mu_{a,m} \cdot \phi_m = \frac{c}{T_m \cdot A_s} \sum_{m=1}^{8192} E_m \cdot \mu_{a,m} \cdot N_m \quad (10)$$

$$X_R = \frac{c}{T_m \cdot A_s} \sum_{m=1}^{8192} Rsp*_m \cdot \mu_{a,m} \cdot E_m \cdot N_m = \frac{Rsp_n \cdot c}{T_m \cdot A_s} \sum_{m=1}^{8192} Rsp_m \cdot \mu_{a,m} \cdot E_m \cdot N_m \quad (11)$$

$$M = \frac{X_A}{X_R} = \frac{Eff_n \cdot \sum_{m=0}^{max} E_m \cdot \mu_{a,m} \cdot N_m}{Rsp_n \cdot \sum_{m=0}^{max} Rsp*_m \cdot E_m \cdot \mu_{a,m} \cdot N_m} = \frac{\psi_1}{Rsp_n \cdot \psi_2} \quad (12)$$

$$\psi_1 = \sum_{m=0}^{max} E_m \cdot \mu_{a,m} \cdot N_m$$

$$\psi_2 = \sum_{m=0}^{max} Eff_m \cdot E_m \cdot \mu_{a,m} \cdot N_m$$

Effective Dose Calculation

The next step is the determination of dose conversion factors (DCFs) that convert the actual exposure rate to effective dose rate. Based on rigorous calculations, the ICRP (1996) has given the rem/R conversion values for various gamma-ray energies and

orientations that are used in the equations to calculate the DCFs. The calculations were performed for all six irradiation geometries as defined by ICRP (1996).

The conversion factors provided by ICRP (1996) convert the air kerma, not the exposure, to effective dose. Therefore, the equations for DCF are different than the equations for M. Air kerma is the sum of initial kinetic energies of all charged ionizing particles produced by photons. ICRP (1996) also provides values to convert a monoenergetic photon flux to an air kerma value. The following values are defined for the equations: F_K (units of pGy cm^2) is the conversion factor of flux to air kerma; F_D (units of Sv/Gy) is the conversion factor of air kerma to effective dose, and ψ_3 is defined to simplify the equations. The effective dose is calculated in Equation 13, and the DCF, which is independent of the detector used since it is for actual exposure rate, is calculated in Equation 14.

$$H = F_D \cdot F_K \cdot \varphi = F_D \cdot F_K \cdot N/T_m \cdot A_s \quad (13)$$

$$DCF = \frac{H}{X_A} = \frac{\sum_{m=1}^{8192} F_{D,m} \cdot F_{K,m} \cdot N_m}{c \cdot \sum_{m=1}^{8192} E_m \cdot \mu_{a,m} \cdot N_m} = \frac{\psi_3}{c \cdot \psi_1} \quad (14)$$

$$\psi_3 = \sum_{m=0}^{\max} F_{D,m} \cdot F_{K,m} \cdot N_m$$

Values for DCF that convert the measured exposure rate from a survey meter to actual effective dose can also be calculated using Equation 15.

$$DCF_{\text{survey meter}} = (DCF \cdot \psi_1)/(\psi_2 \cdot Rsp_n) = DCF \cdot M \quad (15)$$

Measurements

The gamma spectrometer was taken to three different chemical processing plants, owned by three different companies, and three different mine sites, one owned by one company and the other two owned by another company. Chemical plants and mine sites are named by letters to prevent identification of measurements with specific companies. Measurements were also taken of mineralized land at Bradley Junction, of reclaimed mined land at Tenoroc State Park and Rolling Hills, unreclaimed land at Tenoroc (Clay Settling Pond 4), and a baseline at Winter Haven. Gamma energy spectra were also recorded in parking lots or near the gate of the chemical processing plants and the mine sites.

After positioning the spectrometer for measurements, the operator used the laptop computer that controlled the spectrometer to begin measurements. The measurement duration lasted from 10 minutes to 30 minutes, depending on the strength of the radiation field. The higher the radiation field, the less time needed to record a high number of counts. A 90º shielding configuration was used unless otherwise stated. During measurements, two survey meters (Ludlum 12-S and 2401-P) were used to record the

exposure at the detector face as well as the source (the ground for areas such as the gypsum stacks, sand tailings, or concentrated phosphate spill), whenever possible. Readings were also taken with a global positioning unit (unless inside or near a building) and, when possible, pictures were taken. Pictures were not allowed inside the chemical processing plants for security reasons.

After measuring the gamma energy spectra at the chemical processing plants, the rock tunnels and the filter pan areas were determined to be areas of stable radiation fields in which to place dosimeters. The dosimeters were exposed to the radiation fields at or near the same location where the energy spectra were recorded except for tunnels. The dosimeters were placed inside the tunnels, but gamma energy spectra were measured inside only one tunnel. The dosimeters were collected after 19 days (plus or minus one hour) and sent to the vendor to be read. Survey meters were used to measure the exposure rate where the dosimeters were placed when they were installed and when they were collected.

RESULTS

ENERGY SPECTRA ANALYSIS

The gamma energy spectra were evaluated before calculating the conversion factors. Figures 11 and 12 are representative spectra obtained at two different sites. Figure 11 is a spectrum with several peaks that are higher than the low energy band and was measured in a high radiation field (Filter at Plant F). The other spectrum (Clay Settling Pond at Mine Site C) has mostly smaller peaks that are below the low energy band. All spectra recorded had this band of increasing photons counted as energy decreases at low energy, which is a result of the degraded gamma energy spectrum due to photons losing energy interacting with material before reaching the detector. The number of lower energy photons due to Compton scattering reactions occurring inside the detector has been estimated to contribute less than 5% of the total photons. Figures 11 and 12 are of the counts actually recorded by the spectrometer. However, the spectrometer does not count all of the photons that strike it; many of these photons pass through the detector without being recorded. Figures 13 and 14 are of the same spectra after dividing the actual counts by the efficiency curve (performed in the Excel spreadsheet for all spectra) to determine the actual number of photons.

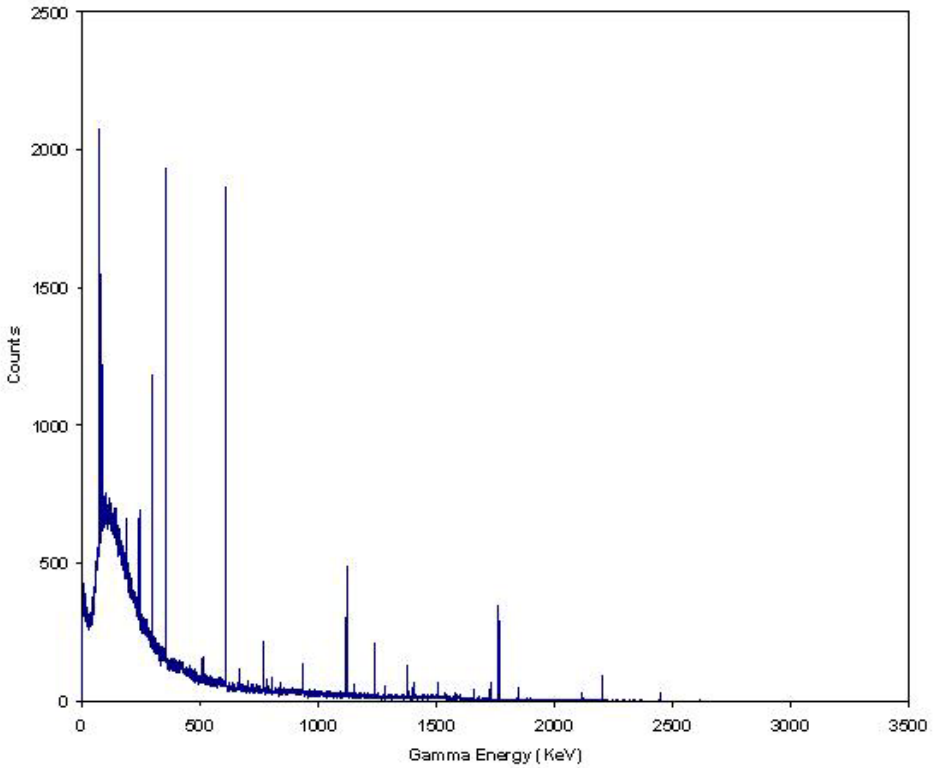

Figure 11. Number of Photons Recorded by the Spectrometer at the Filter of Chemical Processing Plant F.

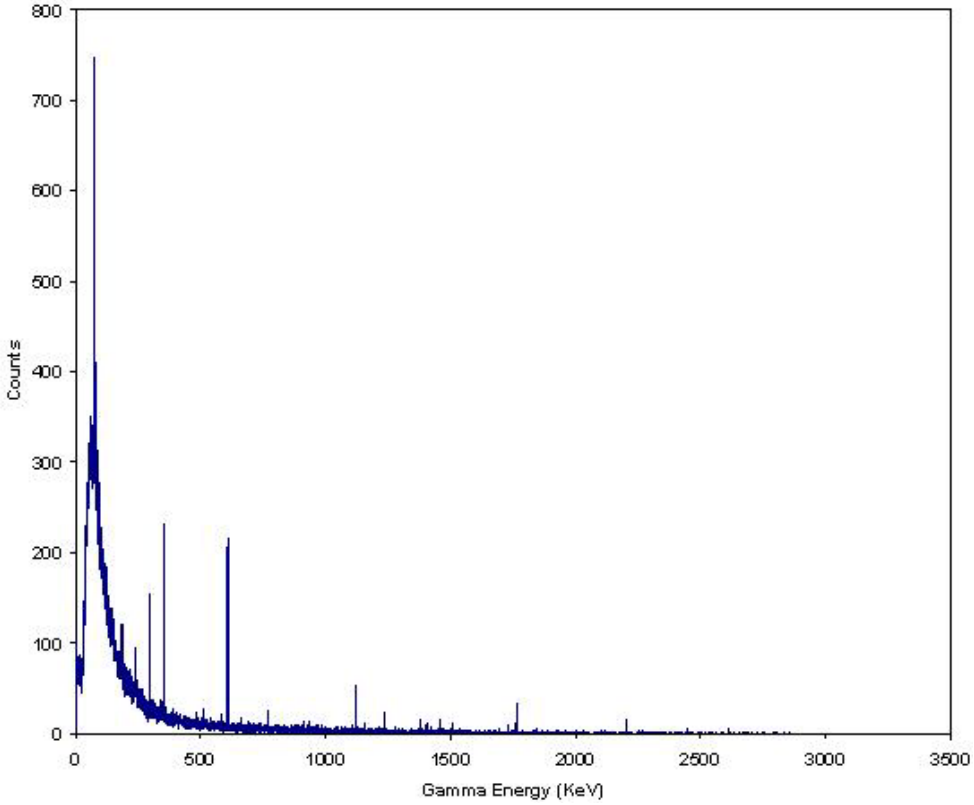

Figure 12. Number of Photons Recorded by the Spectrometer at the Clay Settling Pond at Mine Site C.

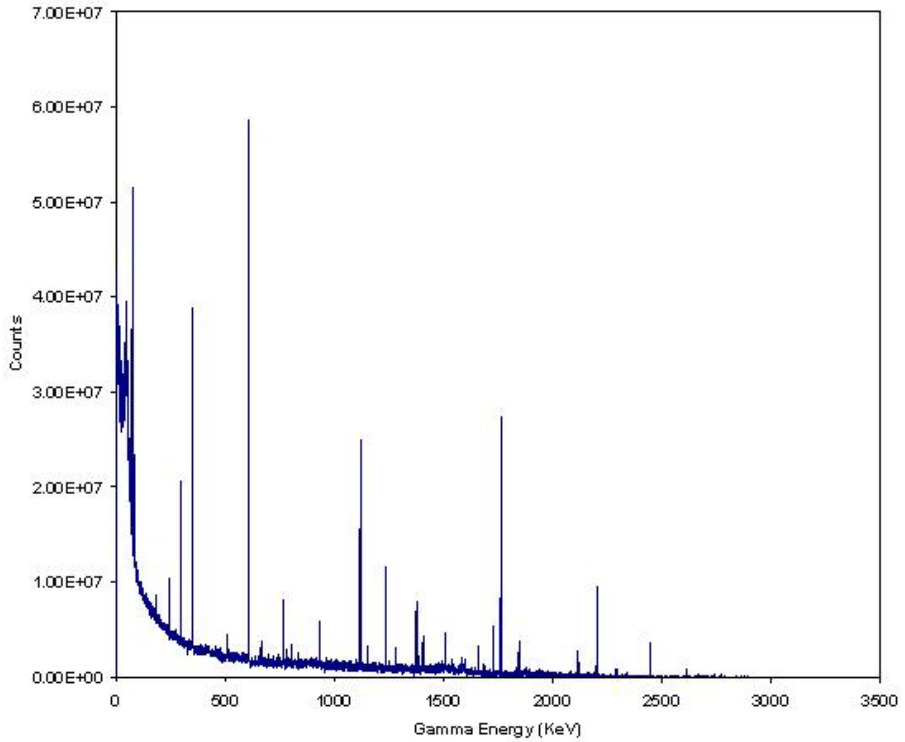

Figure 13. Actual Number of Photons Entering the Front of the Detector at the Filter of Chemical Processing Plant F.

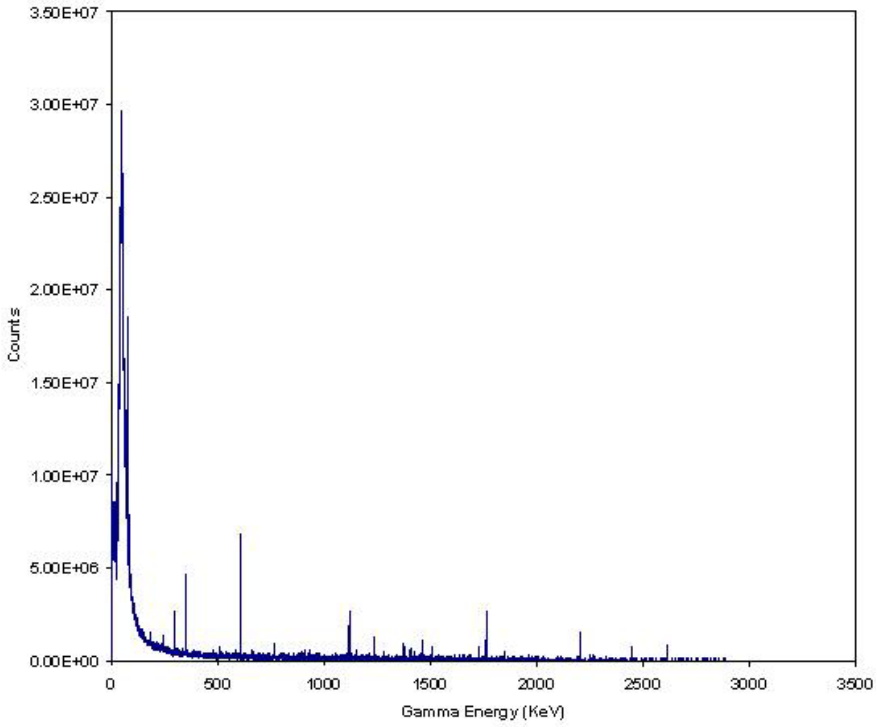

Figure 14. Actual Number of Photons Entering the Front of the Detector at the Clay Settling Pond at Mine Site C.

To understand the spectra better, the actual number of counts has been converted to the total energy of photons per channel as well as the total biological effect (Figures 15 to 18), which is the product of energy flux, AP and kerma conversion factors. The number of photons counted predominate at the lower energies compared to the higher energies (E > 400 keV). The perspective is changed in Figure 15 for the filter, as the total energy (directly related to absorbed dose) is not dominant anymore at photon energies below 400 keV. The low-energy photons still have a large percentage of the total energy measured for the spectrum of the clay settling pond. The biological damage increases the importance of the low-energy photons slightly. Since the response curves for the survey meters have high relative values at low energy compared to high energy, and since the number of photons counted predominate at low energy, it is expected that the exposure value read from the survey meter will be greater than the actual exposure (and, hence, M < 1).

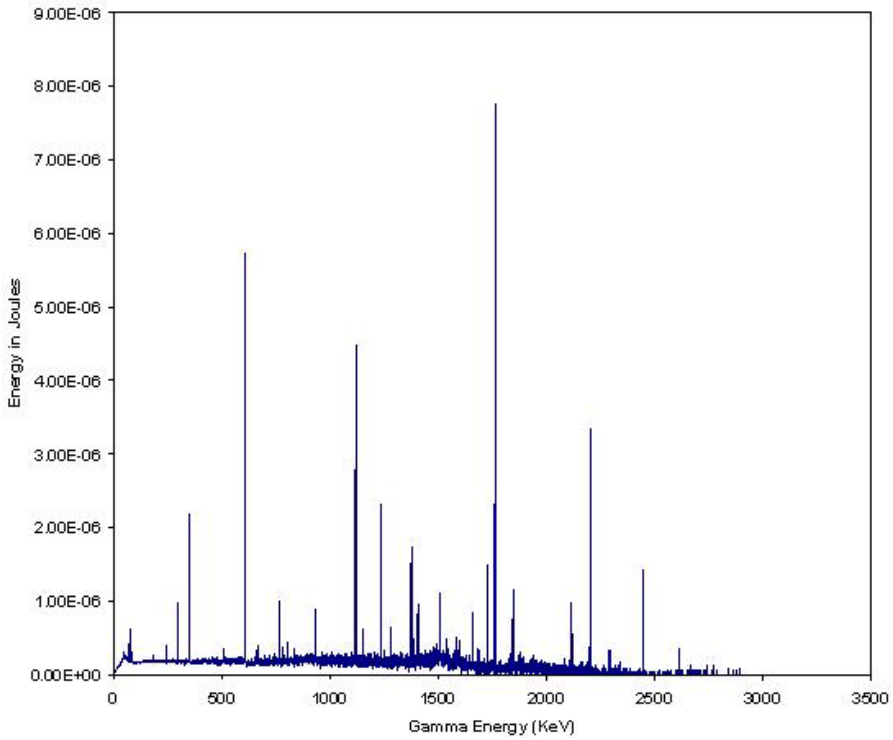

Figure 15. Total Energy Deposited by Gamma Rays as Function of Gamma Energy at Filter of Chemical Processing Plant F.

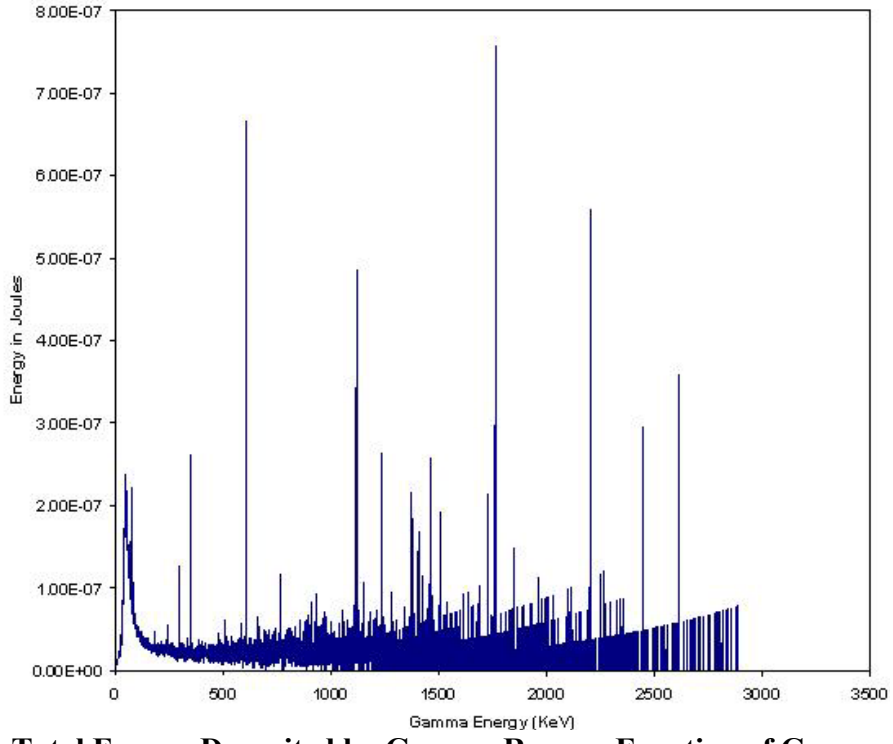

Figure 16. Total Energy Deposited by Gamma Rays as Function of Gamma Energy at the Clay Pond at Mine Site C.

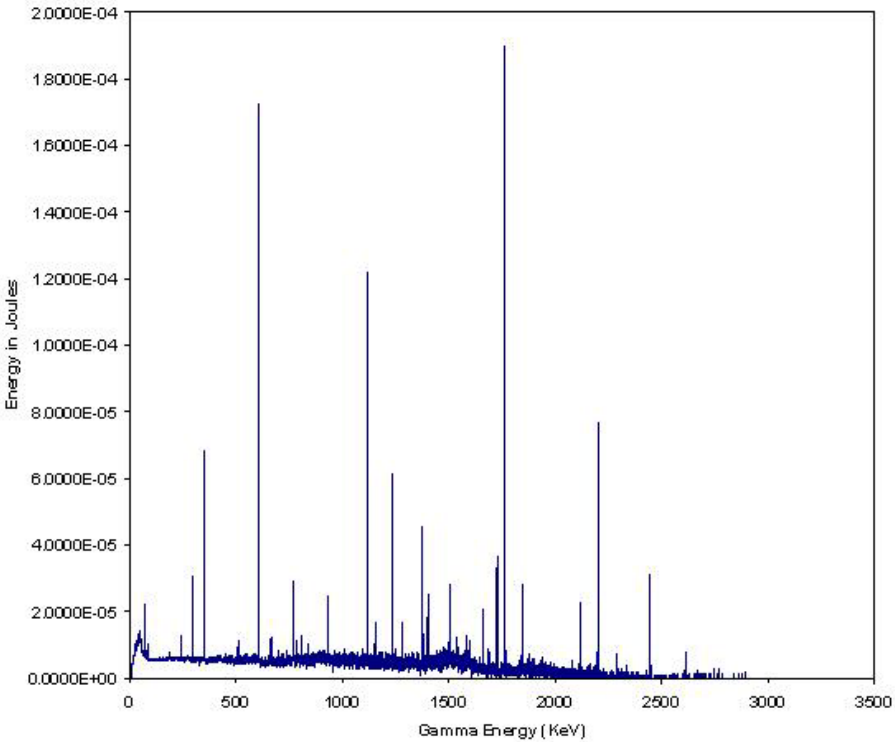

Figure 17. Relative Biological Damage by Gamma Ray as Function of Gamma Energy at the Filter of Chemical Processing Plant F.

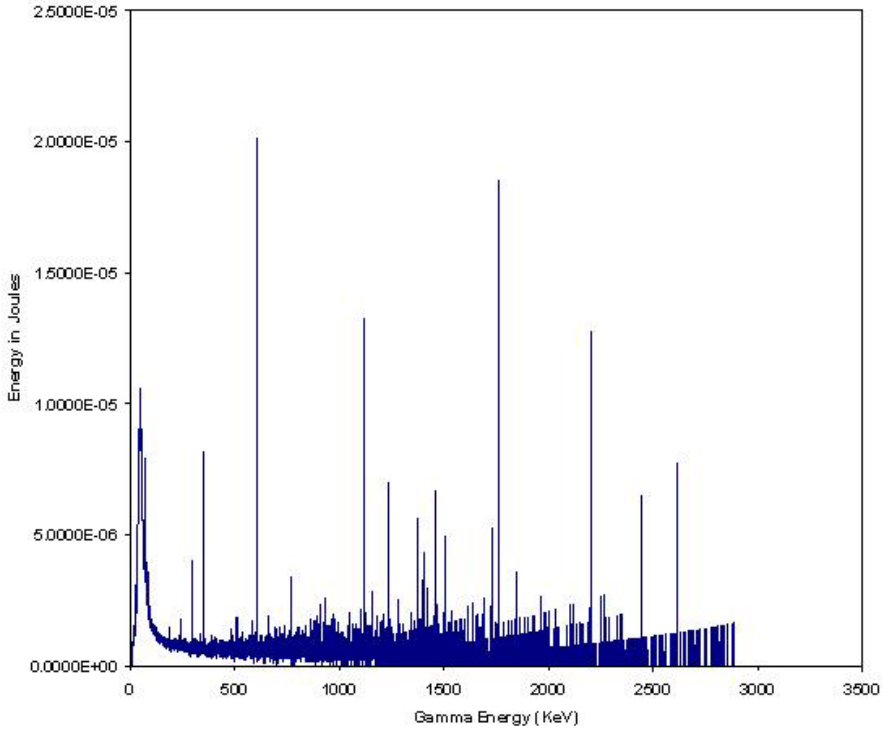

Figure 18. Relative Biological Damage by Gamma Ray as Function of Gamma Energy at the Clay Settling Pond at Mine Site C.

The percentages of total energy deposited per photon energy range are shown in Tables 8 and 9 for the two representative spectra of Filter at Plant F and Clay Settling Pond at Mine Site C. The percentage of energy from the peaks is also presented (total amount of energy deposited from non-degraded photons, which are represented by the energy peaks). From these values, it is seen more quantitatively that even though the number of photons at low energy is greater than at high energy, the high-energy photons are still important due to the higher energy deposited per photon. The "no peaks" values reveal that, although the spectra are dominated by degraded gammas, 16% to 25% of the total energy deposited is from gammas that have not been degraded (have not lost any of their initial energy).

The influence of the gamma photons per energy range on the calculations for M and DCF are also evaluated in Tables 8 and 9 for these two representative spectra. The percent changes in the values of M and DCF are for calculations that exclude the gammas measured in this energy range. (The counts are changed to zero in the Excel spreadsheet.) The conversion factor for the 12-S survey meter is the most sensitive, and the dose conversion factors, independent of the survey meter, are the least sensitive to the measured photon count. The DCF values are independent of the survey meter; survey meter dependent values can be obtained by the product of DCF and M. Only the DCF for the AP orientation is shown since it was the most sensitive of all six orientations.

Table 8. Percentage of Number of Photons, of the Total Energy of the Photons, Change in M, and Change in DCF per Energy Range for the Filter at Chemical Processing Plant F.

Energy (MeV)	% Change				
	Number	Energy	$M_{12\text{-}S}$	$M_{2401\text{-}P}$	DCF_{AP}
0-0.05	24.7	1.5	2.9	1.5	1.8
0-0.5	69.8	21.7	100	2.38	5.31
2 –3	1.4	7.5	3.8	4.4	0.5
1.5 – 3	6.5	27.8	16.0	14.3	2.1
1 – 3	15.6	53.9	37.3	24.7	6.3
0.5 – 3	30.2	78.3	64.2	9.5	19.0
No Peaks Only	9.0	24.7	8.8	4.4	1.1

Table 9. Percentage of Number of Photons, of the Total Energy of the Photons, Change in M, and Change in DCF per Energy Range for the Clay Settling Pond at Mine Site C.

Energy (MeV)	% Change				
	Number	Energy	$M_{12\text{-}S}$	$M_{2401\text{-}P}$	DCF_{AP}
0-0.05	35.3	4.8	7.6	4.7	5.0
0-0.5	85.0	29.7	161	14.0	12.0
2 –3	1.3	11.8	7.1	4.4	0.5
1.5 – 3	3.6	28.1	18.8	14.3	2.1
1 – 3	8.0	50.1	38.4	24.7	6.3
0.5 – 3	15.0	70.3	60.6	9.5	19.0
No Peaks Only	4.6	16.3	9.0	1.3	1.2

Most peaks seen in the spectra are from the U-238 series and include Bi-214, Ra-226 and Pb-214. The majority of the higher energy peaks (> 1 MeV) are from Bi-214. Some peaks from the Th-232 series are seen in the spectra, but at a much smaller abundance. These radioisotopes include Tl-208 (several peaks are seen from Tl-208, but a peak at 583 keV with a large abundance is not seen), Ac-228, and maybe Rn-222, which only has one peak that is shared with a peak from Tl-208.

MINING SITES

Phosphate Ore Matrix Without Overburden

At two of the mine sites, phosphate ore matrix was brought up from the pit by an excavator and placed on the ground by the detector. The spectrometer was moved up to the dumped mine matrix and measurements were recorded (Figure 19). The spectrometer was placed several feet away, despite the reduced intensity of the radiation field due to dilution by distance, to protect the instrument because the matrix was unstable and clumps would fall off during the measurement. Matrix was not measured at the third mine site because the road was impassable for the van carrying the detector due to mud. In addition, the mud also would not allow the detector itself to be positioned next to the dumped matrix. The survey meter readings and the calculated values for M and DCF are presented in Table 10.

Figure 19. Gamma Spectrometer Measuring the Radiation Field of Freshly Dumped Phosphate Ore Matrix.

Table 10. Survey Meter Readings (μR/hr) and Values for M and DCF_A for the Phosphate Ore Matrix.

Site	Survey Meter Reading			
	12-S, detector	2401-P, detector	12-S matrix	2401-P matrix
A	7 ± 1	5 ± 1	13 ± 1	12.5 ± 2.5
B	16 ± 1	20 ± 5	40 ± 2	35 ± 5
Value	12-S	2401-P	Al dosimeter	LiF dosimeter
M, site A	0.529	0.598	0.922	0.962
M, site B	0.497	0.587	0.927	0.958

Site	DCF_A					
	AP	PA	RLAT	LLAT	ROT	ISO
Site A	1.08	0.897	0.642	0.691	0.869	0.729
Site B	1.10	0.902	0.640	0.689	0.872	0.731

Note: Values for M for this and the following tables are for survey meters calibrated with a ^{137}Cs source.

Coarse Phosphate Rock

At Mine Site A, a reading was taken of a large collection of coarse phosphate rock. The detector was pointed towards a long row of piled coarse phosphate rock that was approximately 5 feet high, 3 feet thick, and a few hundred feet long. Furthermore, the ground of the area, on which the detector was placed, also consisted of coarse phosphate rock. The detector was from 83 ± 2 inches away. This is the same rock used throughout the region for asphalt, along railroad tracks, and in parking lots that consists

of pebbles thrown on the grassy ground. The survey meter readings and the calculated values for M and DCF are presented in Table 11.

Table 11. Survey Meter Readings (μR/hr) and Values for M and DCF_A for the Coarse Phosphate Rock at Mine Site A.

Survey Meter Reading					
12-S, detector	2401-P, detector		12-S pile		2401-P pile
50 ± 1	50 ± 10		100 ± 3		95 ± 5
Value M					
12-S	2401-P		Al dosimeter		LiF dosimeter
0.550	0.635		0.928		0.968
DCF_A					
AP	PA	RLAT	LLAT	ROT	ISO
1.07	0.893	0.640	0.687	0.860	0.724

Concentrated Phosphate Spill

At the three mine sites, the gamma energy spectrum was recorded over a spilled concentrated phosphate pile along the conveyor belt of the flotation plant (Figure 20). The pile was typically four to six inches deep. The survey meter readings and the calculated values for M and DCF are presented in Table 12.

Table 12. Survey Meter Readings (μR/hr) and Values for M and DCF_A for the Concentrated Phosphate Spill.

Site	Survey Meter Reading			
	12-S, detector	2401-P, detector	12-S matrix	2401-P matrix
A	24 ± 2	35 ± 5	50 ± 2	65 ± 5
B	78 ± 3	80 ± 10	85 ± 5	100 ± 10
C	82 ± 2	70 ± 10	90 ± 2	100 ± 10

Value	12-S	2401-P	Al dosimeter	LiF dosimeter
M, site A	0.592	0.645	0.922	0.973
M, site B	0.578	0.648	0.924	0.971
M, site C	0.577	0.645	0.924	0.971

Site	DCF_A					
	AP	PA	RLAT	LLAT	ROT	ISO
Site A	1.06	0.889	0.642	0.688	0.855	0.723
Site B	1.06	0.889	0.641	0.687	0.856	0.722
Site C	1.06	0.890	0.641	0.687	0.856	0.723

Figure 20. Spectrometer Measuring Gamma Radiation Emitted by the Pile of Spilled Concentrated Phosphate at a Mining Site.

At Mine Site B, four measurements were taken over the concentrated phosphate spill, each measurement at a different sampling time. These spectra were recorded to determine the error from not collecting enough photon counts. The results are shown in Table 13, which show that the final error is small for M. The values for DCF are not shown here since the errors were smaller than the errors for M.

Table 13. Percent Error from Smaller Measuring Times for M for a Concentrated Phosphate Pile.

Measurement Time (s)	Total Number of Gammas Detected	M		Difference Between M of Longest Counting Time and This Time	
		12-S	2401-P	12-S	2401-P
950.88	8.8×10^9	0.578	0.648	0.0%	0.0%
301.54	2.8×10^9	0.578	0.651	0.0%	0.5%
121.80	1.1×10^9	0.575	0.651	0.5%	0.5%
61.25	5.7×10^8	0.576	0.644	0.3%	0.6%

Sand Tailings

The detector was positioned in the sand tailings area (Figure 21) with the detector pointing down. At Mine Site A, the clay and sand tailings were stored together, so that measurements are of both sand tailings and clay. The survey meter readings and the calculated values for M and DCF are presented in Table 14.

Table 14. Survey Meter Readings (µR/hr) and Values for M and DCF_A for the Sand Tailings Area of the Mine Sites.

Site	Survey Meter Reading			
	12-S, detector	2401-P, detector	12-S, ground	2401-P, ground
A	26 ± 2	25 ± 5	30 ± 2	30 ± 5
B	20 ± 2	25 ± 5	22 ± 2	25 ± 5
C	16 ± 2	10 ± 10	14 ± 2	20 ± 10

Value	12-S	2401-P	Al dosimeter	LiF dosimeter
M, site A	0.554	0.614	0.923	0.966
M, site B	0.565	0.613	0.920	0.968
M, site C	0.552	0.615	0.923	0.966

Site	DCF_A					
	AP	PA	RLAT	LLAT	ROT	ISO
Site A	1.07	0.894	0.642	0.689	0.863	0.726
Site B	1.07	0.893	0.644	0.690	0.861	0.729
Site C	1.08	0.895	0.643	0.690	0.863	0.727

Figure 21. Spectrometer Measuring the Gamma Energy Spectra at the Sand Tailings Area.

Clay Settling Ponds

The detector was positioned beyond the edge of the clay settling ponds. At Mine Site A, the clay and sand tailings were stored together and were dry (no water for settling of clay), so that measurements are of both sand tailings and clay. At Mine Site B, the detector was placed on the soil between two clay settling ponds. Between the two ponds was clay that was not under water. The detector was about six feet away from and pointed at the clay (see Figure 22). At Mine Site C, the settling pond was several feet below the ground level (detector was on top of a dike), and thus the detector had to measure it from several feet away (see Figure 23). The measurement position at Mine Site C was clay that was newly discharged into the settling pond. The survey meter readings and the calculated values for M and DCF are presented in Table 15.

Table 15. Survey Meter Readings (μR/hr) and Values for M and DCF_A for the Clay Settling Ponds of the Mine Sites.

Site	Survey Meter Reading			
	12-S, detector	2401-P, detector	12-S, clay	2401-P, clay
A	26 ± 2	25 ± 5	30 ± 2	30 ± 5
B	25 ± 1	20 ± 10	37 ± 2	30 ± 10
C	30 ± 5	20 ± 5	N/A	N/A

Value	12-S	2401-P	Al dosimeter	LiF dosimeter
M, site A	0.554	0.614	0.923	0.966
M, site B	0.543	0.593	0.921	0.963
M, site C	0.461	0.541	0.926	0.948

Site	DCF_A					
	AP	PA	RLAT	LLAT	ROT	ISO
Site A	1.07	0.894	0.642	0.689	0.863	0.726
Site B	1.08	0.898	0.644	0.691	0.867	0.730
Site C	1.13	0.911	0.642	0.694	0.887	0.740

Figure 22. Spectrometer Measuring the Gamma Radiation Field at the Clay Settling Pond at Mine Site B.

Figure 23. Detector Measuring the Gamma Radiation Field at the Clay Settling Pond at Mine Site C.

CHEMICAL PROCESSING PLANTS

Filter

The detector had to be lifted up four stories using a monorail bridge crane to measure the filters. The floor of the filter area often shook and was wet. Some areas had to be avoided due to water spray, which can damage the spectrometer by causing a short-circuit or voltage leakage from the 3,000 V source. The detector was positioned as close

to the filter as possible (typically, from 10 to 15 feet away) without being sprayed with water. The survey meter readings and the calculated values for M and DCF are presented in Table 16. The filters at Plants D and E were Byrd filters, and the filter at Plant F was a Badger or scroll filter.

Table 16. Survey Meter Readings (μR/hr) and Values for M and DCF_A for the Filters of the Chemical Processing Plants.

Plant	Survey Meter Reading			
	12-S, detector	2401-P, detector	12-S, filter	2401-P, filter
D	160 ± 2	100 ± 10	245 ± 10	275 ± 10
E	23 ± 1	20 ± 10	37 ± 2	35 ± 5
F	115 ± 3	100 ± 10	130 ± 10	130 ± 10

Value	12-S	2401-P	Al dosimeter	LiF dosimeter
M, site D	0.576	0.660	0.927	0.972
M, site E	0.532	0.627	0.926	0.966
M, site F	0.594	0.661	0.926	0.973

Site	DCF_A					
	AP	PA	RLAT	LLAT	ROT	ISO
Site D	1.06	0.889	0.640	0.686	0.854	0.721
Site E	1.07	0.894	0.640	0.687	0.862	0.725
Site F	1.06	0.889	0.641	0.686	0.853	0.721

Reactor

Initially, the plan was to measure the gamma energy spectrum at the roof of the reactor vessel building. Physical limitations prevented us from lifting the detector up to the roof for the measurements, such as lack of a device to lift the detector in one plant and water droplets condensing out of a nearby stack that rained down upon the roof. Measurements of the roof from the floor of the filter area proved futile because the roof was about 20 feet away (below the filter floor) and the relatively strong radiation field from the filter overpowered the radiation field from the roof. By the filter, a gamma energy spectrum recorded with full shielding (0º configuration) showed that sufficient radiation from the filter was penetrating the shielding so that it would be impossible to isolate the roof radiation field, from which the radiation field intensity would have been diluted significantly by distance. Therefore, at Plants D and E, the measurements were recorded at the ground level outside of the concrete, reinforced-steel building that housed the reactor. The detector was only several inches away from the wall. At Plant F, the steel reactor vessel was not in a concrete building and was at the same level as the filter. The detector was placed 6.5 feet away from the reactor vessel, and readings from the survey meter showed that the radiation field from the filter was negligible. The survey meter readings and the calculated values for M and DCF are presented in Table 17.

Table 17. Survey Meter Readings (μR/hr) and Values for M and DCF_A for the Reactor of the Chemical Processing Plants.

Plant	Survey Meter Reading			
	12-S, detector	2401-P, detector		
D	24 ± 2	22 ± 3		
E	30 ± 1	30 ± 5		
F	30 ± 2	25 ± 10		
Value	12-S	2401-P	Al dosimeter	LiF dosimeter
M, site D	0.499	0.573	0.920	0.959
M, site E	0.473	0.546	0.921	0.952
M, site F	0.602	0.652	0.922	0.973

Site	DCF_A					
	AP	PA	RLAT	LLAT	ROT	ISO
Site D	1.09	0.900	0.644	0.692	0.873	0.732
Site E	1.11	0.906	0.644	0.694	0.884	0.736
Site F	1.05	0.888	0.643	0.688	0.854	0.722

Gypsum Stacks

The detector was positioned on top of the gypsum stack, pointing downward onto the hardened part. At Plant F, measurements were taken of the hardened part underneath as well as of some gypsum not yet packed into a hardened form on the side of the "road." The survey meter readings and the calculated values for M and DCF are presented in Table 18.

Table 18. Survey Meter Readings (μR/hr) and Values for M and DCF_A for the Phosphogypsum Stacks of the Chemical Processing Plants.

Plant	Survey Meter Reading			
	12-S, detector	2401-P, detector	12-S, ground	2401-P, ground
D	39 ± 1	30 ± 10	42 ± 1	50 ± 10
E	45 ± 2	40 ± 10	58 ± 2	50 ± 5
F	58 ± 1	45 ± 5	60 ± 1	50 ± 5

Value	12-S	2401-P	Al dosimeter	LiF dosimeter
M, site D	0.570	0.634	0.924	0.970
M, site E	0.586	0.628	0.920	0.969
M, site F, hardened	0.575	0.640	0.925	0.971
M, site F, not hard	0.560	0.623	0.924	0.968

Site	DCF_A					
	AP	PA	RLAT	LLAT	ROT	ISO
D	1.06	0.891	0.642	0.688	0.857	0.724
E	1.06	0.890	0.644	0.690	0.859	0.725
F, hard	1.06	0.891	0.641	0.688	0.857	0.723
F, not hard	1.07	0.893	0.642	0.689	0.860	0.726

Rock Tunnels

The detector was able to be moved into the rock tunnel at Plant D, but not at Plant E and Plant F. Separate measurements were taken in the tunnel at Plant D for ore passing by the belt, ore not passing by the belt, and a composite of both (composite spectrum was measured using a shielding configuration of 180º). The measurements of ore passing by the belt and not passing by the belt are for short duration and were not used in the final calculations of the conversion factors. The values are listed here for qualitative purposes only. The detector was placed outside of the entrance of the tunnel at Plant E, pointing inside. The detector could only approach within 6 feet of the tunnel entrance at Plant F. The survey meter readings and the calculated values for M and DCF are presented in Table 19.

Table 19. Survey Meter Readings (μR/hr) and Values for M and DCF_A for the Rock Tunnel of the Chemical Processing Plants.

Plant	Survey Meter Reading			
	12-S, detector	2401-P, detector	12-S, tunnel	2401-P, tunnel
D, with ore	12 ± 2	20 ± 10	18 ± 2 by ore on belt	N/A
D, with no ore	9.5 ± 0.5	10 ± 5	9 ± 1	10 ± 5
E	40 ± 2	50 ± 5	33 ± 2	30 ± 5
F	18 ± 2	30 ± 5	12 ± 2	10 ± 5

Value	12-S	2401-P	Al dosimeter	LiF dosimeter
M, plant D with ore	0.570	0.634	0.924	0.970
M, plant D, with no ore	0.532	0.644	0.928	0.964
M, plant D, composite	0.532	0.632	0.924	0.964
M, plant E	0.534	0.604	0.922	0.965
M, plant F	0.541	0.582	0.915	0.964

Site	DCF_A					
	AP	PA	RLAT	LLAT	ROT	ISO
D w/ ore	1.10	0.898	0.636	0.687	0.875	0.728
D no ore	1.08	0.895	0.646	0.694	0.870	0.731
D both	1.10	0.897	0.635	0.686	0.873	0.726
E	1.08	0.896	0.643	0.690	0.865	0.728
F	1.08	0.896	0.646	0.693	0.868	0.730

TENOROC STATE PARK

Tenoroc State Park occupies land that once was a mining facility but was partially reclaimed after closure. Measurements at Tenoroc Park were of the sand tailings (Figure 24), rock piles (Figure 25), and Clay Settling Pond 4 (Figure 26). Clay Settling Pond 4 was not reclaimed. Measurements of Clay Settling Pond 3 were not possible due to above-average rainfall in December, which made the approaches to the pond impassable (wet clay), and the clay in the pond was under water. The sand tailings are a grassy area where sand tailings were disposed. The rock pile was where coarse phosphate rock was disposed and is also grassy but with shrubs and trees. The clay at Clay Settling Pond 4 is over 4 feet thick (measured with a rod). Measurements were taken at two different locations for each site. The survey meter readings and the calculated values for M and DCF are presented in Table 20.

Table 20. Survey Meter Readings (µR/hr) and Values for M and DCF_A for Tenoroc State Park.

Plant	Survey Meter Reading			
	12-S, detector	2401-P, detector	12-S, ground	2401-P, ground
Rock pile 1	30 ± 2	20 ± 10	30 ± 2	20 ± 10
Rock pile 2	65 ± 2	50 ± 5	75 ± 2	65 ± 5
Sand tailings 1	23 ± 1	20 ± 10	26 ± 2	30 ± 10
Sand tailings 2	22 ± 2	25 ± 10	24 ± 2	30 ± 10
Clay pond 1	65 ± 5	50 ± 10	75 ± 5	70 ± 10
Clay pond 2	60 ± 3	50 ± 10	68 ± 3	70 ± 10

Value	12-S	2401-P	Al dosimeter	LiF dosimeter
M, rock pile 1	0.506	0.573	0.923	0.958
M, rock pile 2	0.552	0.644	0.928	0.969
M, sand tailings 1	0.557	0.618	0.923	0.967
M, sand tailings 2	0.557	0.604	0.920	0.964
M, clay pond 1	0.548	0.629	0.926	0.967
M, clay pond 2	0.541	0.618	0.926	0.966

Site	DCF_A					
	AP	PA	RLAT	LLAT	ROT	ISO
Rock pile 1	1.10	0.902	0.643	0.692	0.874	0.732
Rock pile 2	1.07	0.892	0.639	0.686	0.858	0.723
Sand tailings 1	1.07	0.893	0.642	0.689	0.862	0.727
Sand tailings 2	1.08	0.894	0.644	0.690	0.864	0.728
Clay pond 1	1.07	0.893	0.640	0.687	0.861	0.725
Clay pond 1	1.08	0.895	0.641	0.688	0.863	0.726

Figure 24. Sand Tailings Area of Tenoroc State Park.

Figure 25. Rock Pile Area of Tenoroc State Park.

Figure 26. Clay Settling Pond 4 of Tenoroc State Park.

BASELINES

Baseline spectra are measurements taken away from mining and processing activities. These sites include mineralized and reclaimed land where people live. Several measurements were taken of Bradley Junction, which is mineralized land. Measurement was also taken at Rolling Hills, which is reclaimed land, at Winter Haven outside the offices of the PCHU, and at Miami outside the offices of the Hemispheric Center for Environmental Technology at Florida International University. Measurements were taken in the grass several feet away from the parking lot unless otherwise stated. The survey meter readings and the calculated values for M and DCF are presented in Table 21.

The descriptions of the sites measured are shown below:

Bradley Junction 1: Detector was in the grass by a parking lot and railroad tracks. Coarse phosphate rock was used as lining of the tracks, which was discovered by the higher exposure reading at the detector level than at the ground level (see Figure 27).
Bradley Junction 2: Detector was in the grass of the yard of a church and rectory. The grass had phosphate pebbles strewn over it to serve as a parking lot.
Bradley Junction 3: The detector was moved about 35 feet away from the position of Bradley Junction 2, deeper into the yard and away from the phosphate pebbles.
Bradley Junction 4: The detector was positioned inside a playground over grass (see Figure 28).
Rolling Hills: The detector was positioned in the back yard of a church.

Table 21. Survey Meter Readings (μR/hr) and values for M and DCF_A for Baselines.

Plant	Survey Meter Reading			
	12-S detector	2401-P detector	12-S, ground	2401-P, ground
Bradley Junction 1	11 ± 1	10 ± 5	15 ± 2	15 ± 5
Bradley Junction 2	38 ± 1	35 ± 5	40 ± 1	35 ± 5
Bradley Junction 3	7 ± 1	5 ± 5	7 ± 1	5 ± 5
Bradley Junction 4	5 ± 1	5 ± 5	7 ± 1	10 ± 5
Rolling Hills	20 ± 2	20 ± 10	22 ± 2	20 ± 10
Winter Haven	7 ± 1	5 ± 5	9 ± 1	12.5 ± 2.5
Miami	4 ± 0.5	N/A	4 ± 0.5	N/A

Value	12-S	2401-P	Al dosimeter	LiF dosimeter
M, Bradley Junction 1	0.552	0.555	0.909	0.961
M, Bradley Junction 2	0.540	0.632	0.927	0.967
M, Bradley Junction 3	0.546	0.551	0.927	0.963
M, Bradley Junction 4	0.574	0.539	0.896	0.964
M, Rolling Hills	0.540	0.586	0.918	0.964
Winter Haven	0.615	0.546	0.892	0.970
Miami	0.561	0.560	0.908	0.928

Site	DCF_A					
	AP	PA	RLAT	LLAT	ROT	ISO
Bradley 1	1.09	0.900	0.650	0.697	0.873	0.736
Bradley 2	1.07	0.893	0.634	0.687	0.861	0.724
Bradley 3	1.08	0.899	0.651	0.698	0.873	0.736
Bradley 4	1.08	0.897	0.656	0.701	0.870	0.738
Rolling Hills	1.08	0.897	0.645	0.692	0.867	0.730
Winter Haven	1.06	0.894	0.658	0.702	0.866	0.736
Miami	1.10	0.892	0.647	0.705	0.907	0.736

Figure 27. Measurement Site of Bradley Junction 1 (Railroad Tracks in the Background).

Figure 28. Measurement Site of Bradley Junction 4.

Parking Lots of Mine Sites and Processing Plants

Gamma energy spectra were recorded in the grass by the parking lots for most of the mining sites and chemical processing plants visited. These measurements were performed after the other measurements had been completed and also provide baseline measurements. Survey meter readings at Mine Site A were higher at the detector level than the ground level, an indicator that a radiation source is present at the side that has a

higher intensity than the ground below. This radiation source was phosphate rocks used in the asphalt of the parking lot. Readings were taken of both the grass area and the asphalt. The measurement at Mine Site C was past the gate on the grassy side by the side of the public road. The radiation exposure was higher at the detector level than the ground level, an indicator that a higher radiation source is present, which was probably phosphate pebbles used in the road. The survey meter readings and the calculated values for M and DCF are presented in Table 22.

Table 22. Survey Meter Readings (μR/hr) and Values for M and DCF_A for Parking Lots of Mining Sites and Processing Plants.

Plant	Survey Meter Reading			
	12-S detector	2401-P detector	12-S, ground	2401-P, ground
Mine Site A, grass	12 ± 2	10 ± 5	9 ± 1	10 ± 5
Mine Site A, asphalt	30 ± 2	N/A	35 ± 2	N/A
Mine Site C	14 ± 2	10 ± 10	7 ± 2	10 ± 10
Plant E	20 ± 2	7.5 ± 2.5	25 ± 2	25 ± 5
Plant F	7 ± 1	10 ± 10	7 ± 1	10 ± 10
Value	12-S	2401-P	Al dosimeter	LiF dosimeter
M, Mine A, grass	0.526	0.534	0.907	0.958
M, Mine A, asphalt	0.570	0.642	0.924	0.971
M, Mine C	0.581	0.565	0.905	0.966
M, Plant E	0.354	0.618	0.962	0.936
M, Plant F	0.534	0.604	0.922	0.965

Site	DCF_A					
	AP	PA	RLAT	LLAT	ROT	ISO
Mine A grass	1.10	0.904	0.651	0.698	0.877	0.739
Mine A asphalt	1.06	0.890	0.641	0.687	0.856	0.723
Mine C	1.07	0.896	0.652	0.698	0.867	0.734
Plant E	1.15	0.910	0.614	0.673	0.888	0.723
Plant F	1.08	0.896	0.643	0.690	0.865	0.728

Parrish Road

Parrish Road is only a few hundred yards long; it is off Route 630, west of Fort Meade, and was built with phosphogypsum. Measurements were taken of this road (Parrish 1), along with another nearby stretch of road constructed using normally utilized material, such as limestone (Parrish 2). The detector was placed on the side of the road to avoid traffic and pointed downward at an angle toward the road. The shielding configuration at this position would ensure only radiation from the road is being detected. The survey meter readings and the calculated values for M and DCF are presented in Table 23.

Table 23. Survey Meter Readings (μR/hr) and Values for M and DCF_A for Parrish Road.

Site	Survey Meter Reading			
	12-S, detector	2401-P, detector	12-S, middle of road	2401-P, middle of road
Parrish 1	16 ± 2	10 ± 5	19 ± 2	20 ± 5
Parrish 2	14 ± 2	10 ± 5	16 ± 1	10 ± 5

Value	12-S	2401-P	Al dosimeter	LiF dosimeter
M, Parrish 1	0.574	0.539	0.896	0.964
M, Parrish 2	0.584	0.608	0.915	0.968

Site	DCF_A					
	AP	PA	RLAT	LLAT	ROT	ISO
Parrish 1	1.08	0.897	0.656	0.701	0.870	0.734
Parrish 2	1.07	0.892	0.646	0.693	0.863	0.727

AVERAGE VALUES AND STANDARD DEVIATIONS OF M AND DCF

The average values and the standard deviations of these values for M and DCF were calculated (Tables 24 and 25) for various groupings. The self-absorbing materials are radioactive materials, which cover a large area, in which the material absorbs most of the gamma radiation emitted. These materials include the stacks, sand tailings, rock pile, concentrated phosphate spills, and clays. Calculations for rock pile, sand tailings, and clays include measurements from the mine sites and Tenoroc State Park.

It is recommended that the values for baseline be used for the surrounding area and the values for "all but baseline" be used for the mines and chemical processing plants. In addition, the values for the stacks, concentrated phosphate spills, clays, and sand tailings should be used for those specific areas due to the lower standard deviation from the average. Average values for other areas were calculated but not shown since their standard deviation is larger than that for "all but baseline." The values for the DCF and for M for the dosimeters are more stable (have lower standard deviation) than the values for M for the survey meters, which is due to the large relative change in response values at low energies in the response curves for the survey meters.

The M value for the PIC was calculated using a representative selection of spectra, which were filter from Plant F, clay from Mine Site C, Bradley Junction 5, concentrated phosphate spill from Mine Site C, and rock tunnel from Plant F. The error range for the average value of M is twice the standard deviation: $M_{PIC} = 1.107 \pm 0.004$.

Table 24. Average Values of M for Various Groupings and the Standard Deviation Shown as ± 2 σ.

Grouping	12-S	2401-P	Al dosimeter	LiF TLD
All	0.55 ± 0.09	0.60 ± 0.08	0.92 ± 0.02	0.96 ± 0.02
Baselines	0.58 ± 0.06	0.56 ± 0.06	0.91 ± 0.02	0.96 ± 0.01
All but baseline	0.55 ± 0.07	0.62 ± 0.06	0.92 ± 0.06	0.97 ± 0.01
Filter	0.57 ± 0.06	0.65 ± 0.04	0.93 ± 0.01	0.97 ± 0.01
Reactor	0.52 ± 0.02	0.59 ± 0.11	0.91 ± 0.04	0.96 ± 0.02
Self-absorbing	0.55 ± 0.06	0.62 ± 0.05	0.92 ± 0.01	0.97 ± 0.01
Stacks	0.57 ± 0.02	0.63 ± 0.02	0.92 ± 0.01	0.97 ± 0.01
Sand Tailings	0.56 ± 0.02	0.62 ± 0.01	0.92 ± 0.01	0.97 ± 0.01
Rock Pile	0.54 ± 0.05	0.62 ± 0.08	0.92 ± 0.01	0.96 ± 0.01
Concentrated phosphate spill	0.58 ± 0.02	0.65 ± 0.01	0.92 ± 0.01	0.97 ± 0.01
Clay	0.53 ± 0.08	0.60 ± 0.07	0.92 ± 0.01	0.96 ± 0.01

Note: The values are for survey meters calibrated with a ^{137}Cs source. The survey meter 2401-P used in the study has an additional Rsp_n value of 1.3. Therefore, the meter-specific value of M for the 2401-P used in this study is M* = M/1.3.

Table 25. Average Values of DCF for Various Groupings and the Standard Deviation Shown as ± 2 σ.

Grouping	AP	PA	RLAT	LLAT	ROT	ISO
All	1.08 ± .04	0.89 ± .01	0.64 ± .01	0.69 ± .01	0.87 ± .02	0.73 ± .01
Baselines	1.08 ± .02	0.90 ± .01	0.65 ± .01	0.70 ± .01	0.87 ± .01	0.73 ± .01
All but baseline	1.07 ± .04	0.89 ± .01	0.64 ± .01	0.69 ± .01	0.86 ± .02	0.73 ± .01
Filter	1.06 ± .02	0.89 ± .01	0.64 ± .01	0.69 ± .01	0.86 ± .01	0.72 ± .01
Reactor	1.09 ± .06	0.90 ± .02	0.64 ± .01	0.69 ± .01	0.87 ± .03	0.73 ± .01
Self-absorbing	1.07 ± .02	0.89 ± .01	0.64 ± .01	0.69 ± .01	0.86 ± .02	0.73 ± .01
Stacks	1.06 ± .01	0.89 ± .01	0.64 ± .01	0.69 ± .01	0.86 ± .01	0.72 ± .01
Sand Tailings	1.07 ± .01	0.89 ± .01	0.64 ± .01	0.69 ± .01	0.86 ± .01	0.73 ± .01
Rock Piles	1.08 ± .03	0.90 ± .01	0.64 ± .01	0.69 ± .01	0.86 ± .02	0.73 ± .01
Conc. Phos. spill	1.06 ± .01	0.89 ± .01	0.64 ± .01	0.69 ± .01	0.86 ± .01	0.72 ± .01
Clay	1.09 ± .05	0.90 ± .02	0.64 ± .01	0.69 ± .01	0.87 ± .02	0.73 ± .01

DOSIMETER RESPONSES

The exposure rates for the locations where the dosimeters were placed are shown in Table 26 for both when the dosimeters were installed and collected. The average of the two readings is calculated and used to determine the total exposure to the dosimeters. The exposure is converted to effective dose by multiplying by M and DCF for the AP

position. The values for the dosimeters are also adjusted by the value of M. However, the dosimeter companies employ proprietary algorithms to read the measured dose values, which include determining if the gamma energy is low or high and adjusting respectively for the dosimeter response. The error reported is from both the standard deviation of the M and DCF values as well as the error range of the survey meter reading. The 2401-P meter was calibrated with Ra-226, so Rsp_n of 1.3 is used in the calculations.

The dosimeter vendor subtracts out the background using a controlled dosimeter, but since the control dosimeter was below the minimum detection limit, it is assumed that no background subtraction was performed. The background will, therefore, not be subtracted from the calculated exposure. A background reading of 7 μR/hr for the 12-S and 5 μR/hr for the 2401-P can be used if background was subtracted (1.4 mR for the 12-S and 1.2 for the 2401-P for 19 days).

The reading for rock tunnel for Plant D was 15 μR/hr for ore on belt and 9 μR/hr for no ore using the 12-S. This value was averaged since the belt was empty approximately one-half of the time. At the filter of Plant E, the filter membrane had been removed (and a new one installed) and was on the floor near the dosimeter. An increase in the measured exposure was observed. From Table 26, it can be seen that for all filter measurements, differences between installation and collection doses are observed. The Mylar window of the ICN LiF TLD in the filter areas has fallen off, but this window is for measuring beta particles. The dosimeters from the filter areas were coated with phosphogypsum scale after 19 days.

Table 26. Measured Exposure and Dose and Calculated Effective Dose Values.

	Rock Tunnel			Filter		
	Plant D	Plant E	Plant F	Plant D	Plant E	Plant F
Exposure Rate (μR/hr)						
12-S, install	12 ± 1	33 ± 2	10 ± 2	245 ± 5	37 ± 2	130 ± 10
12-S collect	13 ± 1	34 ± 3	10 ± 1	230 ± 10	50 ± 3	105 ± 3
2401-P, install	10 ± 5	30 ± 5	10 ± 5	275 ± 25	35 ± 5	130 ± 10
2401-P, collect	10 ± 5	30 ± 10	15 ± 5	230 ± 20	55 ± 5	100 ± 10
Calculated Total Effective Dose for AP Position (mrem)						
12-S	1.5 ± 0.5	9.0 ± 1.3	2.7 ± 0.6	64 ± 8	12 ± 2	32 ± 4
2401-P	2.4 ± 2.6	7.0 ± 4	2.9 ± 2.8	59 ± 15	11 ± 3	28 ± 7
Measured Dose in mrem (± 1 mrem)						
AlO dosimeter	< 1	8.8 ± 1	< 1.1 ± 1	89.93 ± 1	6.7 ± 1	40.39 ± 1
LiF TLD	< 10	< 10	< 10	63.66 ± 6	< 10	27.30 ± 3
Corrected Dose (mrem)						
AlO dosimeter	< 1 ± 1	7.7 ± 1	1 ± 1	88 ± 3	6.3 ± 1.5	38.2 ± 1.5
LiF TLD	< 10	< 10	<10	70 ± 9	< 10	31 ± 5

For the AlO dosimeter, effective dose agreements between the survey meter and AlO dosimeter are within the error ranges for the rock tunnels. The effective dose values derived from the survey meters are lower than the effective doses measured by the AlO dosimeters for the filter areas but approximately equal to the effective doses measured by the LiF dosimeters. The filter results of Plant E should not be used due to the filter change-out.

The calculation of responses of one detector over another is performed by using the values of M. The M value is an inverse of the response of the detector to the total radiation field. Therefore, the ratio of the AlO dosimeter over the PIC detector (AlO/PIC) is M_{PIC}/M_{AlO} = 1.107/0.92 = 1.20 ± 0.01 (two standard deviations). This value is lower than the measured value from Birky and others (1998), which was 1.53 ± 0.88 (two standard deviations), but is within the error range. However, it must be noted that the value of M_{AlO} does not include vendor-applied algorithms to convert the measured dose to an effective dose. In addition, another source of uncertainty in this ratio is the potential of a different response curve between the old X9 dosimeter used in 1998 and the new Luxel dosimeter used in 2003. The AlO/PIC ratio, using the measured exposure values from the survey meters for the filter areas (and converting the actual exposure to a PIC measured exposure by dividing by M_{PIC}) and the measured effective dose from the AlO dosimeter (not the corrected dose using M_{AlO}) is 1.5 ± 0.7 for the 12-S and 1.6 ± 1.2 for the 2401-P. These ratios are approximately equal to the measured ratio in Birky and others (1998). The ratio is near 1.0 for the rock tunnel at Plant E, which had a lower dose than the filter areas.

The value of the ratio of the aluminum dosimeter over the LiF TLD (AlO/LiF), using values for "all but baseline," is equal to M_{LiF}/M_{AlO} = 0.97/0.92 = 1.05, which is lower than the measured value of 1.22 ± 0.30 (two standard deviations) from Birky and others (1998). Again, vendor-applied algorithms and the new AlO dosimeter from Landauer may affect the comparison of these results. The AlO/LiF ratio using the measured dose for the filter areas (not corrected by using M_{AlO} or M_{LiF}) is 1.40 ± 0.15, which is higher than the value from Birky and others (1998), but is within the uncertainty range.

CONCLUSIONS AND RECOMMENDATIONS

The gamma energy spectra of the phosphate industry are characterized by an increasing number of photons as the photon energy decreases. Therefore, the response behavior of survey meters, PIC, and dosimeters are increasingly important at low energy levels. The survey meters 12-S and 2401-P have a relatively high response in this energy range, resulting in a conversion factor M of 0.55 and 0.62, respectively. Measurements taken with these meters, if calibrated with Cs-137 or Ra-226, over-respond to the radiation field. A common practice in the phosphate industry is to calibrate the survey meter to a PIC at several spots in the phosphate mine or plant. This practice should result in a Rsp_n value that will bring the response of the survey meter closer to the actual exposure value. However, the response of the PIC decreases as energy decreases past 90 keV, which results in a conversion factor M of 1.11. Therefore, the PIC under-responds to the radiation field by approximately 10%.

The conversion of exposure to effective dose is possible using the dose conversion factors calculated in this report, most of which are less than the actual exposure (except for AP). The product of the F_D and F_K, which converts photon flux to effective dose, drops continually as the photon energy decreases (see Figure 29), which when coupled with the increasing number of photons at lower energies, results in the R-to-rem conversion factor being below 1. The exception is the AP position.

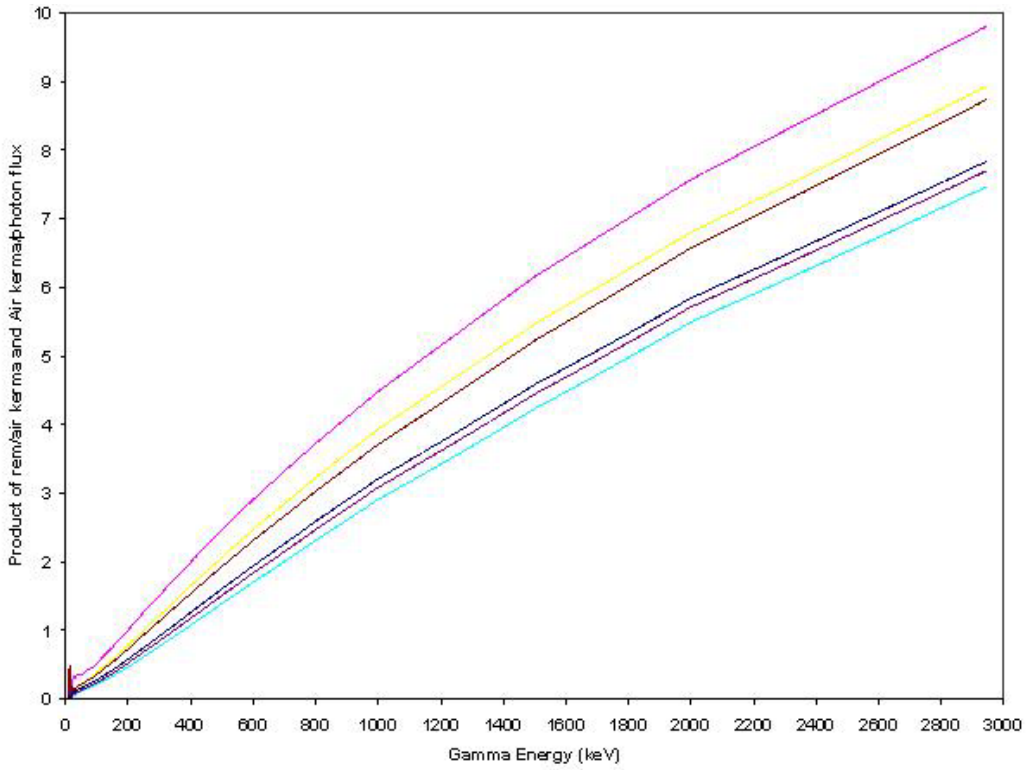

Figure 29. Values of the Conversion Factors that Convert Air Kerma to Rem (order of curves from top to bottom is AP, PA, ROT, ISO, LLAT and RLAT).

A main uncertainty in these calculations, due to the increased importance of low energy gamma photons, is the lack of information for the efficiency and response of the survey meters, dosimeters, PIC and the gamma spectrometer at low gamma energy. The radioisotope source with the lowest energy main gamma is Am-241, with a gamma energy of 59.5 keV. The efficiency of many detectors below 59.5 keV is based on modeling and curve fitting. The extent of the error resulting from this uncertainty is not possible to calculate but is estimated to be small since the energies and the R-to-rem conversion factors are low at these low photon energies. Uncertainty also exists at high photon energies for the survey meters since the highest data point in the efficiency curves is 1260 keV. Further investigation of the response of the survey meters is recommended to obtain more accurate response curves for these calculations. Higher energy and low energy sources would be required from sources other than radioisotopes, which would be difficult to achieve.

The change in the AlO dosimeter design from Landauer has introduced a source of uncertainty in comparing the calculated values of this report and the measured values of the 1998 report. Further investigation is recommended in determining the different responses between the old and the new design or performance of an extensive evaluation of the new AlO dosimeter dose values compared to PIC and LiF TLD similar to the evaluation done by Birky and others (1998) for the old AlO dosimeter. Attempts to obtain old dosimeters to compare with the new dosimeters were not successful. In addition, to test the accuracy of these calculations, measurements could be performed versus dosimeters and exposures measured by survey meters calibrated against a PIC per the standard procedure of the phosphate industry. Since the vendor-applied algorithms are proprietary, the phosphate industry could use these results in private consultation with the dosimeter vendor to incorporate the measured gamma energy spectra into algorithms that account for the dosimeter energy-dependent response.

REFERENCES

Anagnostakis M, Hinis E, Karangelos D, Petropoulos N, Rouni P, Simopoulos S, Žunić Z. 2001. Determination of depleted uranium in environmental samples by gamma-spectroscopic techniques. Archive of Oncology 9(4): 231-6.

Birky B, Tolaymat T, Warren B, Bolch WE, Ammons R, McNally T, Nall JW. 1998. Evaluation of exposure to Technologically Enhanced Naturally Occurring Radioactive Materials (TENORM) in the phosphate industry. Bartow (FL): Florida Institute of Phosphate Research. FIPR Publication nr 05-046-155.

Cember H. 1987. Introduction to health physics. 2nd ed. Elmsford (NY): Pergamon Press.

Colaresi J (Product Manager, Detector Products Division, Canberra). 2002 Sep 17. E-mail communication.

El-Dine N, El-Shershaby A, Ahmed F, Abdel-Haleem A. 2001. Measurement of radioactivity and radon exhalation rate in different kinds of marbles and granites. Applied Radiation and Isotopes 55: 853-60.

Ennis M, Trubey DK. 1992. Effective gamma ray dose equivalent for specific radionuclides. Oak Ridge (TN): Oak Ridge Information Center, Oak Ridge National Laboratory. Publication nr DLC-164/UNGER.

Florida Institute of Phosphate Research. 1998. 1998-2003 strategic research programmatic and management priorities. Bartow (FL): Florida Institute of Phosphate Research.

Hamlat M, Djeffal S, Kadi H. 2001. Assessment of radiation exposures from naturally occurring radioactive materials in the oil and gas industry. Applied Radiation and Isotopes 55: 141-6.

Han HJ, Reece WD, Kim CH. 1999. Improved estimates of effective dose equivalent using two optimal anisotropic responding dosimeters. Health Phys. 77: 536-40.

Hipkin J, Paynter RA, Shaw PV. 1998. Exposures at work to ionising radiation due to the use of naturally occurring radioactive materials in industrial processes. Appl. Radiat. Isot. 49(3): 205-9.

ICN. 2003 Jan 7. Fax from representative of ICN Worldwide Dosimetry Service, 3300 Hyland Ave, Costa Mesa, CA 92626.

International Commission on Radiological Protection (ICRP). 1977. Recommendations of the International Commission on Radiological Protection. Oxford: Pergamon Press. ICRP Publication nr 26.

International Commission on Radiological Protection. 1987. Data for use in protection against external radiation. Oxford: Pergamon Press. ICRP Publication nr 51.

International Commission on Radiological Protection. 1991. Recommendations of the International Commission on Radiological Protection. Oxford: Pergamon Press. ICRP Publication nr 60.

International Commission on Radiological Protection (ICRP). 1995. Smith H, ed. Conversion coefficients for use in radiological protection against external radiation. New York: Pergamon Press. ICRP Publication nr 74.

Kim CH, Reece WD, Postoni JR, Sr. 1998. Effective dose equivalent and effective dose for photon exposures from point and disk sources on the floor. Health Phys. 75: 170-8.

Landauer. 2003 Jan 6. E-mail from representative of Landauer.

Ludlum. 2002 Sep 18. Fax from representative of Ludlum Measurements, Inc., 501 Oak Street, Sweetwater, TX 79556.

RSA Publications. 2000. RadCalc, version 1.1g, Hebron CT.

Saito K, Petoussi N, Zankl M, Viet R, Jacob P, Drexler G. 1991. Organ dose as a function of body weight for environmental gamma rays. J. Nucl. Sci. Technol. 28: 627.

Saito K, Petoussi-Hess N, Zankl M. 1998. Calculation of the effective dose and its variation from environmental gamma ray sources. Health Phys. 74: 698-706.

Schleien B, Slaback LA, Birky BK. 1998. Handbook of health physics and radiological health. Baltimore (MD): Williams & Wilkins.

Smith KP, Blunt DL, Williams GP, Tebes CL. 1996. Radiological dose assessment related to management of naturally occurring radioactive materials generated by the petroleum industry. Argonne (IL): Argonne National Laboratory, Environmental Assessment Division. Publication nr ANL/EAD-2.

Tsoulfanidis N. 1983. Measurement and detection of radiation. New York: Hemisphere Publishing Corporation.

Tsutsumi M, Saito K, Moriuchi S. 2000. Development of a detector for measuring effective dose (equivalent) for external photon exposures in natural environment. Journal of Nuclear Science and Technology 37(3): 300-6.

United Nations Scientific Committee on the Effects of Atomic Radiation. 1977. Source and effects of ionizing radiation: 1977 report to the General Assembly, with annexes. New York: United Nations.

United Nations Scientific Committee on the Effects of Atomic Radiation. 1988. Sources, effects and risks of ionizing radiation: 1988 report to the General Assembly, with annexes. New York: United Nations.

United Nations Scientific Committee on the Effects of Atomic Radiation. 2000. Source and effects of ionizing radiation: 2000 report to the General Assembly, with annexes. New York: United Nations.

Zankl M, Petoussi N, Drexler G. 1992. Effective dose and dose equivalent: the impact of the new ICRP definition for external photon irradiation. Health Phys. 62: 395.

Zankl M, Fill U, Petoussi-Hess N, Regulla D. 2002. Organ dose conversion coefficients for external photon irradiation of male and female voxel models. Phys. Med. Biol. 47 (14): 2367-85.

APPENDIX: SURVEY METER DOSE CONVERSION FACTORS

The ICRP (1977 and 1991) has defined various quantities for radiation safety, such as absorbed dose, equivalent dose (and dose equivalent), and effective dose (effective dose equivalent). Absorbed dose is the amount of energy absorbed by a unit mass of material due to radiation. The equivalent dose is calculated by multiplying the absorbed dose, which is averaged over a tissue or organ, and the radiation weighting factor for each radiation exposure event. The effective dose is the sum of the weighted equivalent doses (obtained by multiplying tissue equivalent doses by tissue weighting factors) for various tissues that represent, in total, the human body. Absorbed dose is expressed in units of Gray (SI unit) or rad; equivalent and effective dose are expressed as Sieverts (SI units) or rems.

The ICRP (1996) has published a table of dose conversion factors for exposure to monoenergetic photons that convert the photon energy to an effective dose. These conversion factors were calculated using extensive Monte Carlo numerical modeling for six different orientations of the irradiating gamma rays to the human body. The six orientations are described below:

- Antero-posterior geometry (AP): Ionizing radiation strikes the body in an orthogonal direction to the person's long axis.
- Postero-anterior geometry (PA): Ionizing radiation strikes the back of the body in an orthogonal direction to the person's long axis.
- Right lateral geometry (RLAT): Ionizing radiation strikes the body on the right side in an orthogonal direction.
- Left lateral geometry (LLAT): Ionizing radiation strikes the body on the left side in an orthogonal direction.
- Rotational geometry (ROT): The body is irradiated by a parallel beam of ionizing radiation in an orthogonal direction to the person's long axis and rotates around the long axis at a uniform rate.
- Isotropic geometry (ISO): The body is irradiated by a radiation field in which the particle fluence per unit of solid angle is independent of direction.

When a person is standing on a large affected area like a dry clay pond site, sand tailings area, or reclaimed land, the ISO geometry is probably most appropriate. Under conditions of multiple surrounding sources and frequent worker movement, the ROT geometry may be more appropriate. Under conditions of a smaller fixed source and fairly constant worker position, one of the other geometries, e.g., AP for a worker facing a source, can be chosen.

The dose conversion factors determined in this study are presented below in Table A-1 for actual exposure (independent of the survey meter), in Table A-2 for the 12-S survey meter (converts measured exposure to effective dose) and in Table A-3 for the 2401-P survey meter. The values are for the baseline (surrounding region) and for the phosphate industry.

Table A-1. Average Values of DCF (Actual Exposure to Effective Dose) for Various Groupings and the Standard Deviation Shown as ± 2 σ.

Grouping	AP	PA	RLAT	LLAT	ROT	ISO
Baselines	1.08 ± .02	0.90 ± .01	0.65 ± .01	0.70 ± .01	0.87 ± .01	0.73 ± .01
Industry	1.07 ± .04	0.89 ± .01	0.64 ± .01	0.69 ± .01	0.86 ± .02	0.73 ± .01

Table A-2. Average Values of DCF for the 12-S Survey Meter for Various Groupings and the Standard Deviation Shown as ± 2 σ.

Grouping	AP	PA	RLAT	LLAT	ROT	ISO
Baselines	0.62 ± .06	0.52 ± .06	0.37 ± .06	0.40 ± .06	0.51 ± .06	0.42 ± .06
Industry	0.59 ± .07	0.49 ± .07	0.35 ± .07	0.38 ± .07	0.47 ± .02	0.40 ± .01

Table A-3. Average Values of DCF for the 2401-P Survey Meter for Various Groupings and the Standard Deviation Shown as ± 2 σ.

Grouping	AP	PA	RLAT	LLAT	ROT	ISO
Baselines	0.60 ± .06	0.50 ± .06	0.36 ± .06	0.39 ± .06	0.49 ± .06	0.41 ± .06
Industry	0.66 ± .06	0.55 ± .06	0.40 ± .06	0.43 ± .06	0.53 ± .06	0.45 ± .06